Climate Model Downscaling in Central Asia: A Dynamical and a Neural Network Approach

Bijan Fallah[1], Christoph Menz[1], Emmanuele Russo[2], Paula Harder[3], Peter Hoffmann[1], Iulii Didovets[1], Masoud Rostami[1,5], and Fred F. Hattermann[1,4]

[1]Potsdam Institute for Climate Impact Research (PIK), P.O. Box 601203, 14412 Potsdam, Germany

[2]ETH Zürich, Department of Environmental Systems Science, Universitätstrasse 16, 8092 Zürich, Switzerland

[3]Mila Quebec AI Institute, Montreal, Canada

[4]Eberswalde University for Sustainable Development (HNEE), Germany

[5]Laboratoire de Météorologie Dynamique (LMD), Sorbonne University (SU), Ecole Normale Supérieure (ENS), Paris, France

Correspondence: Bijan Fallah (fallah@pik-potsdam.de)

Abstract. To estimate future climate change impacts, usually high-resolution climate projections are necessary. Statistical and dynamical downscaling or a hybrid of both methods are mostly used to produce input datasets for impact modelers. In this study, we use the regional climate model (RCM) COSMO-CLM (CCLM) version 6.0 to identify the added value of dynamically downscaling a general circulation model (GCM) from the sixth phase of the Coupled Model Inter-comparison Project (CMIP6) and its climate change projections' signal over Central Asia (CA). We use the MPI-ESM1-2-HR (at 1° spatial resolution) to drive the CCLM (at 0.22° horizontal resolution) for the historical period of 1985-2014 and the projection period of 2019-2100 under three different shared socioeconomic pathways (SSPs): SSP1-2.6, SSP3-7.0 and SSP5-8.5 scenarios. Using the Climate Hazards Group InfraRed Precipitation with Station data (CHIRPS) gridded observation dataset as reference, we evaluate the performance of CCLM driven by ERAInterim reanalysis over the historical period. CCLM's added value, compared to its driving GCM, is significant (more than 5mm/day) over CA mountainous areas, which are at higher risk of extreme precipitation events. Additionally, we employ the CCLM to refine future climate projections. We present high-resolution maps of heavy precipitation changes based on CCLM and compare them with CMIP6 GCMs ensemble. Our analysis shows a significant increase in heavy precipitation intensity and frequency over CA areas that are already at risk of extreme climatic events in the present day. Finally, we train a convolutional neural network (CNN) to map a GCM simulation to its dynamically downscaled CCLM. We show that the CNN could emulate the GCM-CCLM model chain over large CA areas. This emulator has added

This page contains no comments

values when applied to a new GCM-CCLM model chain. [1]Scientific communities interested in downscaling CMIP6 models could use our downscaling data. The CNN architecture can be applied as an alternative to dynamical and statistical methods.

1 Introduction

The increasing global mean temperature due to anthropogenic greenhouse gas emissions presents a significant challenge for society, requiring the assessment and prediction of future impacts on human health, natural ecosystems, and economies across different regions of the world (Allan et al., 2021). Regional studies on vulnerability, impacts, and adaptation necessitate reliable high-resolution climate projections, which are typically achieved through dynamical downscaling via Regional Climate Models (RCMs) (Rummukainen, 2010; Feser et al., 2011), statistical techniques (Maraun and Widmann, 2018; Fowler et al., 2007), or a hybrid of both approaches (Maraun et al., 2015; Meredith et al., 2018; Laflamme et al., 2016).

Central Asia (CA), recognized as one of the most vulnerable regions to climate change impacts, is heavily dependent on water resources from glaciers and rivers that are shrinking due to rising temperatures and decreasing precipitation (Reyer et al., 2017; Fallah et al., 2023; Didovets et al., 2024; Fallah and Rostami, 2024). The area faces significant challenges to food security, characterized by declining crop yields and an increased occurrence of severe and frequent extreme weather events like floods and landslides. These conditions damage infrastructure, livelihoods, and agriculture, resulting in population displacement and migration (Allan et al., 2021; Reyer et al., 2017).

[2]Despite these critical concerns, the development of high-resolution climate projections in CA is impeded by the significant uncertainties inherent in the existing high-resolution observational and reanalysis datasets (Fallah et al., 2016a).[4][5]Dynamical downscaling of CMIP6 models for the CA region is vital for accurately simulating extreme convective precipitation events, which are influenced by the orography of the region, large-scale atmospheric circulation, and sea surface temperature anomalies in the Indian Ocean and the Pacific (Kendon et al., 2014; Demory et al., 2020; Xu et al., 2022). [3]Dynamical downscaling enhances the resolution of a driving GCM and produces a robust, physically consistent regional state of the climate. [6]High-resolution atmospheric models have been shown to have better skills over complex topographies in estimating variables like precipitation than in situ observations, satellite-derived and radar datasets (Lundquist et al., 2019). Many studies confirm that RCMs can better represent small-scale atmospheric features, especially for precipitation over complex topographies (Ban et al., 2015; Wang et al., 2013; Frei et al., 2003). This method is often preferred over statistical downscaling approaches, which assume that present statistical relationships will hold in the future (Hess et al., 2022). However, RCMs are computationally demanding and inherit a 'cascade of uncertainty', meaning that the uncertainties in the models will expand from one step or chain to another, highly affecting RCM outcomes and must be considered prior to performing climate projections (Mitchell and Hulme, 1999; Sørland et al., 2018). [8]Despite these considerations, the added value of RCMs concerning their driving GCM is constantly debated in the community and is highly dependent on the driving GCM (Jacob et al., 2012; Lenz et al., 2017; Fotso-Nguemo et al., 2017; Di Luca et al., 2012, 2015). [10]An RCM is tuned to perform over the target local region. However, a GCM is tuned to represent energy and water balance globally (Sørland et al., 2018).

[7]

Number: 1 Author: anonymous   Subject: Comment on Text   Date: 05.06.2024, 14:01:01
this sentence is a bit weak and should, when kept, go before the CNN is mentioned.

Number: 2 Author: anonymous   Subject: Comment on Text   Date: 05.06.2024, 14:01:01
This paragraph and the one that follows need restructuring. The first should be: pros and cons of dynamical downscaling. And the second should be: the added value of RCMs for central asia (i.e., the research gap you're trying to fill). Right now it feels all mixed up. So for the second paragraphs there shouldn't be any vague sentences about dynamical downscaling in general, but what it brings to use it on CA.

Number: 3 Author: anonymous   Subject: Pencil   Date: 05.06.2024, 14:01:01

Number: 4 Author: anonymous   Subject: Highlight   Date: 05.06.2024, 14:01:01
This feels strange seeing how you haven't introduced what CMIP6 models are before. You first need to introduce CMIP6.

Author: anonymous   Subject: Sticky Note Date: 05.06.2024, 14:01:01
Also it doesn't follow from the previous sentence.

Number: 5 Author: anonymous   Subject: Inserted Text   Date: 05.06.2024, 14:01:01
One option to complement these datasets is to use dynamical downscaling with RCMs..

Number: 6 Author: anonymous   Subject: Highlight   Date: 05.06.2024, 14:01:01
These two sentences say the same thing.

Number: 7 Author: anonymous   Subject: Pencil   Date: 05.06.2024, 14:01:01

Number: 8 Author: anonymous   Subject: Cross-Out   Date: 05.06.2024, 14:01:01
"Because", you just listed cons so that would lead to why the added value is debated.

Number: 9 Author: anonymous   Subject: Cross-Out   Date: 05.06.2024, 14:01:01

Number: 10   Author: anonymous   Subject: Highlight   Date: 05.06.2024, 14:01:01
This again is a pros and cons, and feels out of place. You can remove this.

Various international institutions have collaborated within the Coordinated Regional Climate Downscaling Experiment (CORDEX) to address these issues and improve the models' inter-comparability. CORDEX aims to create a better framework for producing climate projections at a regional scale that is suitable for impact evaluation and adaptation planning globally, aligned with the timeline of the Intergovernmental Panel on Climate Change Sixth Assessment Report (Kikstra et al., 2022). However, most CORDEX research focuses on highly industrialized countries (Allan et al., 2021; Taylor et al., 2012). No simulation (except this study) driven by the CMIP6 model simulations has been planned so far for CORDEX-CA (see https://wcrp-cordex.github.io/simulation-status/CMIP6_downscaling_plans.html, last visited on 17.04.2024). Sadly, developing countries, including CA, bear the brunt of global warming's consequences, with only a limited number of CORDEX model simulations available for this region (Naddaf, 2022). The dynamical downscaling in CA can provide detailed insights into regional climate phenomena often not captured by coarser-resolution global models (Russo et al., 2019). Climate projections might be sensible to different parameter settings, emphasizing the need for careful calibration and validation of regional models. Dynamical downscaling's added value lies in its ability to tailor climate projections more closely to regional specifics, thereby improving the utility of climate data for regional climate change impact assessments (Russo et al., 2020). Despite some systematic biases, dynamical downscaling consistently provides high-quality datasets that accurately describe the climatology of all climate variables in CA (Qiu et al., 2022).

Beyond dynamical methods, recent developments in machine learning, including CNNs as the most popular choice, offer promising and potentially transformative avenues for statistical downscaling (Harder et al., 2023; Rampal et al., 2024). CNNs have proven effective in numerous earth science disciplines besides downscaling, such as classification (Gardoll and Boucher, 2022), segmentation (Galea et al., 2024) and prediction (Watson-Parris et al., 2022) thanks to their capacity to extract features from spatial data and identify non-linear relationships between inputs and outputs. CNNs can recognize and encode spatial hierarchies in data (Zhu et al., 2017), making them exceptionally suitable for geospatial data, which is fundamental in climate modelling. Unlike traditional statistical methods that often require manual selection and careful engineering of features, CNN automatically learn the most predictive features directly from the data (Reichstein et al., 2019). CNNs can model complex non-linear relationships between input data and outputs, often present in climate data due to intricate interactions in weather systems. CNNs are generally more straightforward and efficient for tasks that aim to predict or classify based on patterns distributed across the spatial domain, such as temperature or precipitation patterns in climate models (Racah et al., 2017). CNNs are adept at maintaining spatial coherence in the output, which is critical in downscaling where preserving the geographical patterns of climate variables (like precipitation) is crucial (Kurth et al., 2018). Constrained CNNs integrate physical constraints or laws directly into the training process. The constraining is done by changing the loss function or the network's architecture to enforce compliance with physical laws (i.e., conservation of mass, energy, or momentum). Unconstrained CNNs operate without explicitly incorporating physical laws or constraints into the network's architecture or loss functions. They focus solely on learning from the input data to the output predictions based on the data-driven patterns they detect. This study explores unconstrained and constrained CNN approaches to understand their effectiveness in downscaling and how they perform when applied to GCMs on which they were not initially trained.

The research questions guiding this study are:

Number: 1 Author: anonymous   Subject: Pencil   Date: 05.06.2024, 14:01:01

Number: 2 Author: anonymous   Subject: Comment on Text   Date: 05.06.2024, 14:01:01
which models? The RCMs?

Number: 3 Author: anonymous   Subject: Pencil   Date: 05.06.2024, 14:01:01

Number: 4 Author: anonymous   Subject: Cross-Out   Date: 05.06.2024, 14:01:01

Number: 5 Author: anonymous   Subject: Cross-Out   Date: 05.06.2024, 14:01:01

Number: 6 Author: anonymous   Subject: Inserted Text   Date: 05.06.2024, 14:01:01
Specifically,

Number: 7 Author: anonymous   Subject: Cross-Out   Date: 05.06.2024, 14:01:01

Number: 8 Author: anonymous   Subject: Comment on Text   Date: 05.06.2024, 14:01:01
just before you said that no simulation has been done for CA by CORDEX? If you mean driver by other GCMs then you need to say that.

Number: 9 Author: anonymous   Subject: Cross-Out   Date: 05.06.2024, 14:01:01

Number: 10   Author: anonymous   Subject: Cross-Out   Date: 05.06.2024, 14:01:01
Out of context.

Number: 11   Author: anonymous   Subject: Comment on Text   Date: 05.06.2024, 14:01:01
This feels like it should be before, when you list the pros and cons of RCMs.

Number: 12   Author: anonymous   Subject: Highlight   Date: 05.06.2024, 14:01:01
Again this feels weird seeing how you just said that there's only a very limited number of cordex simulations..

Number: 13   Author: anonymous   Subject: Cross-Out   Date: 05.06.2024, 14:01:01

Number: 14   Author: anonymous   Subject: Comment on Text   Date: 05.06.2024, 14:01:01
Acronym not introduced before... It's not enough if it's mentioned in the abstract, it needs to be done again in the introduction.

Number: 15   Author: anonymous   Subject: Inserted Text   Date: 05.06.2024, 14:01:01
Convolutional Neural Networks (CNNs)

Number: 16   Author: anonymous   Subject: Pencil   Date: 05.06.2024, 14:01:01
This paragraph feels messy. Try to avoid starting every sentences by CNNs ... otherwise it won't feel natural.

Number: 17   Author: anonymous   Subject: Cross-Out   Date: 05.06.2024, 14:01:01

Number: 18   Author: anonymous   Subject: Comment on Text   Date: 05.06.2024, 14:01:01
There should not be a new paragraph after this, seeing how it's the same purpose. Remove line break.

Number: 19   Author: anonymous   Subject: Highlight   Date: 05.06.2024, 14:01:01

Number: 20   Author: anonymous   Subject: Cross-Out   Date: 05.06.2024, 14:01:01

Number: 21   Author: anonymous   Subject: Inserted Text   Date: 05.06.2024, 14:01:01
s

Number: 22   Author: anonymous   Subject: Cross-Out   Date: 05.06.2024, 14:01:01
Said just above.

Number: 23   Author: anonymous   Subject: Comment on Text   Date: 05.06.2024, 14:01:01
More straightforward and efficient than what? Which other models?

Number: 24   Author: anonymous   Subject: Cross-Out   Date: 05.06.2024, 14:01:01

Various international institutions have collaborated within the Coordinated Regional Climate Downscaling Experiment (CORDEX) to address these issues and improve the models' inter-comparability. CORDEX aims to create a better framework for producing climate projections at a regional scale that is suitable for impact evaluation and adaptation planning globally, aligned with the timeline of the Intergovernmental Panel on Climate Change Sixth Assessment Report (Kikstra et al., 2022). However, most CORDEX research focuses on highly industrialized countries (Allan et al., 2021; Taylor et al., 2012). No simulation (except this study) driven by ~~the~~ CMIP6 ~~model simulations~~ has been planned so far for CORDEX-CA (see https://wcrp-cordex.github.io/simulation-status/CMIP6_downscaling_plans.html, last visited on 17.04.2024). ~~Sadly,~~ developing countries, including CA, bear the brunt of global warming's consequences, with only a limited number of CORDEX model simulations available for this region (Naddaf, 2022). ~~The~~ dynamical downscaling in CA can provide detailed insights into regional climate phenomena often not captured by coarser-resolution global models (Russo et al., 2019). ~~Climate projections might be sensible to different parameter settings, emphasizing the need for careful calibration and validation of regional models.~~ Dynamical downscaling's added value lies in its ability to tailor climate projections more closely to regional specifics, thereby improving the utility of climate data for regional climate change impact assessments (Russo et al., 2020). Despite some systematic biases, dynamical downscaling consistently provides high-quality datasets that accurately describe the climatology of all climate variables in CA (Qiu et al., 2022).

Beyond dynamical methods, recent developments in machine learning, including CNNs ~~as the most popular choice,~~ offer promising ~~and potentially transformative~~ avenues for statistical downscaling (Harder et al., 2023; Rampal et al., 2024). CNNs have proven effective in numerous earth science disciplines besides downscaling, such as classification (Gardoll and Boucher, 2022), segmentation (Galea et al., 2024) and prediction (Watson-Parris et al., 2022) thanks to their capacity to extract features from spatial data and identify non-linear relationships between inputs and outputs.

CNNs can recognize and encode spatial hierarchies in data (Zhu et al., 2017), making them exceptionally suitable for geospatial data, which is fundamental in climate modelling. Unlike traditional statistical methods that often require manual selection and careful engineering of features, CNN automatically learns the most predictive features directly from the data (Reichstein et al., 2019). ~~CNNs can model complex non-linear relationships between input data and outputs, often present in climate data due to intricate interactions in weather systems.~~ CNNs are generally more straightforward and efficient for tasks that aim to predict or classify based on patterns distributed across the spatial domain, such as temperature or precipitation patterns in climate models (Racah et al., 2017). CNNs are adept at maintaining spatial coherence in the output, which is critical in downscaling where preserving the geographical patterns of climate variables (like precipitation) is crucial (Kurth et al., 2018). [25] Constrained CNNs integrate physical constraints or laws directly into the training process. [26] ~~he constraining is done~~ by changing the loss function or the network's architecture to enforce compliance with physical laws (i.e., conservation of mass, energy, or momentum). Unconstrained CNNs operate without explicitly incorporating physical laws or constraints [27] ~~to the network's architecture or loss functions.~~ [28] They focus solely on learning from the input data to the output predictions based on the data-driven patterns they detect. This study explores unconstrained and constrained CNN approaches to understand their effectiveness in downscaling and how they perform when applied to GCMs on which they were not initially trained.

The research questions guiding this study are:

– Research Question 1: How effectively can CMIP6 models be downscaled for the CORDEX Central Asia region to enhance precipitation simulations?

– Research Question 2: Can convolutional neural networks [1](CNNs) effectively downscale GCM outputs, and how do they perform when applied to GCMs they were not initially trained on?

The manuscript will focus on three [3]main topics: [2]-added value of [4]CLM for the representation of precipitation over CA, 2-dynamical downscaling[5] gnal of CCLM for heavy precipitation and 3-training a CCLM emulator using a CNN. We present data and methods in section 2. The results of dynamical and hybrid downscaling are introduced in section 3 and 4, respectively. Finally, we discuss the results and draw conclusions in section 5.

2 Data and methods

The schematic shown in figure 1) depicts the methodology used in this study. In the following we will explain it in more details.

2.1 Employed Models and Experimental Setups

2.1.1 RCM

In our study, we conduct a series of simulations with the COnsortium for Small scale Modelling in CLimate Mode (CCLM) RCM. CCLM is a regional climate model developed by the German Weather Service (DWD) and the German Climate Computing Center (Deutsches Klimarechenzentrum, DKRZ) from the COSMO numerical weather prediction model (Rockel and Geyer, 2008), widely used for short-term weather forecasting. [6]~~he original core of COSMO-CLM or CCLM, was called Local~~ ~~MOdel (LM), developed by DWD for weather forecasting. The adopted LM version for climate purposes formed the CCLM~~ ~~(Böhm et al., 2003).~~ CCLM is designed to simulate [7]the regional climate [8]at high spatial resolution, allowing researchers to study various aspects of the climate system, such as temperature, precipitation, and extreme events. CCLM has been utilized in numerous studies to evaluate the impact of climate change on various regions, including Europe (Russo et al., 2021), Africa (Panitz et al., 2014; Dosio and Panitz, 2016), and Asia (Jacob et al., 2014; Kotlarski et al., 2014; Wang et al., 2013). It has also been used for climate projection studies and to assess the effectiveness of climate adaptation and mitigation strategies. The model has been thoroughly evaluated and validated (Fallah et al., 2016b; Russo et al., 2019; Kjellström et al., 2011). Its ability to produce realistic simulations of the current climate and its variability has made it one of the most widely used regional climate models in the scientific community (Sørland et al., 2021).

For our experiments, we used a[9] similar model set-up as the "optimal" set-up provided in the study of Russo et al. (2019). The CORDEX protocol requires a set of simulations that can be divided into two main groups. The first one, referred to as the evaluation run, consists of a single model experiment performed over the period 1979-2014, using ERAInterim at a spatial resolution of T255 ($\sim 0.7°$) as the driving data. In the second[10] ~~eam~~ (projection), the models[11] ~~ust~~ run with boundary conditions from GCMs of the CMIP6 project for the period 1950-2100 under different [12]SSPs (here, we have chosen a single GCM: MPI-ESM1-2-HR and SSP126, SSP370 and SSP585 scenarios). SSPs are baseline scenarios describing the future development

Number: 1 Author: anonymous Subject: Cross-Out Date: 05.06.2024, 14:01:01

Number: 2 Author: anonymous Subject: Comment on Text Date: 05.06.2024, 14:01:01
these two topics sound the same.

Number: 3 Author: anonymous Subject: Comment on Text Date: 05.06.2024, 14:01:01
consistency: later when you list things, you use 1), 2) and 3) not 1-, 2-, etc. Choose one

Number: 4 Author: anonymous Subject: Comment on Text Date: 05.06.2024, 14:01:01
this was not introduced in the introduction...

Number: 5 Author: anonymous Subject: Cross-Out Date: 05.06.2024, 14:01:01

Number: 6 Author: anonymous Subject: Cross-Out Date: 05.06.2024, 14:01:01
Not sure this is necessary.

Number: 7 Author: anonymous Subject: Cross-Out Date: 05.06.2024, 14:01:01

Number: 8 Author: anonymous Subject: Comment on Text Date: 05.06.2024, 14:01:01
how much?

Number: 9 Author: anonymous Subject: Comment on Text Date: 05.06.2024, 14:01:01
Is this what is described afterwards? If yes, should be made clear by: "this means that ...". Otherwise you need to say what the optimal set up is.

Number: 10 Author: anonymous Subject: Cross-Out Date: 05.06.2024, 14:01:01
"step"

Number: 11 Author: anonymous Subject: Cross-Out Date: 05.06.2024, 14:01:01
"is"

Number: 12 Author: anonymous Subject: Comment on Text Date: 05.06.2024, 14:01:01
new acronym

pathways depending on population, technology and economic growth, urbanization, investment in healthcare and education, land use and energy (Riahi et al., 2017).

We have chosen the two available CORDEX-CA evaluation simulations from other models, driven by ERAInterim at 0.22° horizontal resolution, for comparison/evaluation of our RCM simulations, which are driven by ERAInterim for the evaluation period. The two simulations are 1) ERAInterim-RMIB-UGent-ALARO-0 (Giot et al., 2016) and 2) ERAInterim-GERICS-REMO2015 (Jacob and Podzun, 1997; Fotso-Nguemo et al., 2017).

2.1.2 CNNs

We create an emulator of CCLM using a CNN. We use the output of the CCLM Version 6.0 RCM, which is driven by the MPI-ESM1-2-HR GCM under four different scenarios (for 2019-2100). Historical is based on the data of greenhouse gas levels, land use, and other climate forcings from 1850 to 2014 that were observed. SSP126 represents a "green" future where global resources are protected, human well-being is improved, and income gaps are narrowed. This scenario has low challenges to adaptation and low greenhouse gas emissions. Challenges to adaptation refer to the degree of difficulty that societies might face in adjusting to the environmental, economic, and social impacts of climate change. Specifically, this term refers to a society's fundamental susceptibility and the accessibility and efficacy of technologies and approaches designed to lessen the impacts of climate change. The adaptation challenges are minimal in the SSP126 scenario, which envisions a sustainable future. This implies that, under this scenario, global cooperation and sustainable practices lead to advancements in technology and governance that significantly reduce vulnerability to climate change impacts. Additionally, societal structures are resilient, and resources are managed to minimise environmental stresses and maximise human well-being. SSP370 depicts a regional rivalry future where nationalism and regional conflicts prevail, global issues are ignored, and inequality is increasing. This scenario has high challenges to adaptation and high greenhouse gas emissions. SSP585 portrays a fossil-fueled development future where global markets are connected, technological progress is fast, but environmental policies are weak. This scenario has low challenges to adaptation and very high greenhouse gas emissions. As an additional dataset, we merge the ERA-Interim reanalysis and CCLM simulation driven by it (ERAInterim-CCLM) to our previous data pool of GCM and RCM (see Fig. 1). We then train our CNN model based on the architecture proposed by Harder et al. (2023), which can incorporate physical constraints to ensure mass conservation and energy balance. We evaluate our model in the CA domain. We have to note that we use not the whole GCM domain as input for the CNN but only the domain covering the CA (Fig. 3).

In the context of deep learning for climate modelling, the 'perfect model' approach involves starting with high-resolution data, which is considered accurate or nearly perfect, and intentionally degrading it to a lower resolution. The aim is to simulate a scenario where the 'truth' (the original high-resolution data) is known, and then to recover this high-resolution from the artificially degraded data using deep learning techniques. This approach is a crucial part of training, as it teaches the model the desired mapping from low to high resolution, enabling the model to effectively learn how to upscale or enhance resolution while minimizing the loss of critical information. It's a controlled experiment that helps refine the model's capabilities.

Number: 1 Author: anonymous Subject: Pencil Date: 05.06.2024, 14:01:01

Number: 2 Author: anonymous Subject: Cross-Out Date: 05.06.2024, 14:01:01

Number: 3 Author: anonymous Subject: Cross-Out Date: 05.06.2024, 14:01:01
mentioned above.

Number: 4 Author: anonymous Subject: Cross-Out Date: 05.06.2024, 14:01:01

Number: 5 Author: anonymous Subject: Cross-Out Date: 05.06.2024, 14:01:01

Number: 6 Author: anonymous Subject: Pencil Date: 05.06.2024, 14:01:01

Number: 7 Author: anonymous Subject: Highlight Date: 05.06.2024, 14:01:01
This has no place here and should be before when you introduce the ssps.

Number: 8 Author: anonymous Subject: Cross-Out Date: 05.06.2024, 14:01:01
"add"

Number: 9 Author: anonymous Subject: Cross-Out Date: 05.06.2024, 14:01:01

Number: 10 Author: anonymous Subject: Comment on Text Date: 05.06.2024, 14:01:01
Reference to Figure 2?

Number: 11 Author: anonymous Subject: Inserted Text Date: 05.06.2024, 14:01:01
(*corresponding Zenodo repository at https://zenodo.org/records/8150694 (last visited on 21st of June 2023))*

Number: 12 Author: anonymous Subject: Cross-Out Date: 05.06.2024, 14:01:01
"As input of the CNN, we take the part of the GCM that covers CA, and its predictions are also evaluated over the CA domain."

Number: 13 Author: anonymous Subject: Cross-Out Date: 05.06.2024, 14:01:01

Number: 14 Author: anonymous Subject: Pencil Date: 05.06.2024, 14:01:01

Number: 15 Author: anonymous Subject: Cross-Out Date: 05.06.2024, 14:01:01
. The

Number: 16 Author: anonymous Subject: Inserted Text Date: 05.06.2024, 14:01:01
there are two possible ways to train the CNN: 1) the perfect and 2) imperfect model framework.

Number: 17 Author: anonymous Subject: Cross-Out Date: 05.06.2024, 14:01:01

Number: 18 Author: anonymous Subject: Cross-Out Date: 05.06.2024, 14:01:01
upscaling

Number: 19 Author: anonymous Subject: Inserted Text Date: 05.06.2024, 14:01:01
The machine learning model is then trained to reproduce the high-resolution data, while receiving this artificial low-resolution input.

Number: 20 Author: anonymous Subject: Cross-Out Date: 05.06.2024, 14:01:01
upscaled

Number: 21 Author: anonymous Subject: Cross-Out Date: 05.06.2024, 14:01:01

Number: 22 Author: anonymous Subject: Cross-Out Date: 05.06.2024, 14:01:01

The "imperfect model" approach, on the other hand, acknowledges that both the low-resolution (GCM output) and the high-resolution (RCM output) datasets have their inherent errors and limitations. In this scenario, we do not have a single source of truth but rather two separate sets of data:

- Low-resolution data: [2] ~~This~~ may capture global or large-scale phenomena but miss regional details (Xu et al., 2021; Chokkavarapu and Mandla, 2019).

- High-resolution data: [3] ~~This~~ provides detailed regional information but may still have errors or not perfectly reflect reality due to limitations in data collection, model configuration, or computational constraints (Muttaqien et al., 2021).

In this setup, the challenge for [4] ~~deep learning~~ is to learn a mapping between these two independently imperfect data sets. [5] ~~With using~~ the CNN [6] ~~we try to train a model that can~~ predict high-resolution details from low-resolution inputs as accurately as possible despite the absence of a perfect ground truth. This involves understanding and modeling the uncertainties and biases inherent in both datasets.

[7] Many regions of CA receive low precipitation throughout the year and the spatio-temporal variability of precipitation is large. One needs a large dataset of GCM output and the corresponding RCM with various precipitation patterns for training a CNN to find an RCM emulator that captures the mapping from GCM to RCM.

[8] ~~First~~, the [10] ~~daily~~ datasets are shuffled randomly. We then [9] ~~have~~ used a total number of 68141 (60%), 22714 (20%) and 22714 (20%) RCM simulation days for training, validation and testing, respectively. The low-resolution (GCM) and high-resolution (RCM) datasets have 30×60 and 120×240 grid points over latitudes and longitudes, respectively. Therefore, the downscaling factor (N) is 4 in this case. [11] ~~For a complete explanation of the CNN architecture, we refer to the work of Harder et al. (2023) and the corresponding Zenodo repository at https://zenodo.org/records/8150694 (last visited on 21st of June 2023).~~

[1][12] Figure 2 shows the schematic of the standard CNN (without constraint layers) architecture used for two times up-sampling in this study. We briefly explain the steps shown in the schematic:

- Conv (Convolutional Layer): [13] ~~Initially,~~ these layers help [14] extracting various levels of features from the low-resolution images, such as edges, textures, and other relevant image details.

- ReLU (Rectified Linear Activation Unit): This non-linear activation function [15] ~~a key player in our model's learning process. It~~ introduces non-linearity, outputting the input directly if it's positive; otherwise, it outputs zero. This [16] ~~intriguing~~ function helps the network learn complex patterns efficiently.

- TransConv (Transposed Convolutional Layer): This layer is crucial for [17] ~~the task of~~ upscaling. It increases the spatial dimensions of the feature maps, performing a sort of learned interpolation. This [18] ~~reassures us about~~ the model [19] ~~s~~ ability to add details to the upscaled images based on the features extracted and processed in the earlier layers.

- ResBlock (Residual Block): They allow the model to learn corrections [20] ~~(or residuals)~~ to the [21] primary interpolated outputs, refining the details and adding [23] high-frequency information that enhances the [22] ~~perceptual~~ quality of the upscaled images. [24] Adding original input features (from earlier layers) to the output of several convolutional layers ensures that no critical information is lost during processing.

Number: 1 Author: anonymous   Subject: Pencil   Date: 05.06.2024, 14:01:01

Number: 2 Author: anonymous   Subject: Cross-Out   Date: 05.06.2024, 14:01:01

Number: 3 Author: anonymous   Subject: Cross-Out   Date: 05.06.2024, 14:01:01

Number: 4 Author: anonymous   Subject: Cross-Out   Date: 05.06.2024, 14:01:01
"the CNN"

Number: 5 Author: anonymous   Subject: Cross-Out   Date: 05.06.2024, 14:01:01

Number: 6 Author: anonymous   Subject: Cross-Out   Date: 05.06.2024, 14:01:01
"is trained to"

Number: 7 Author: anonymous   Subject: Comment on Text   Date: 05.06.2024, 14:01:01
Feels out of place, should go before you say that you merge different datasets i.e. line 135

Number: 8 Author: anonymous   Subject: Cross-Out   Date: 05.06.2024, 14:01:01
"Before training"

Number: 9 Author: anonymous   Subject: Cross-Out   Date: 05.06.2024, 14:01:01

Number: 10   Author: anonymous   Subject: Comment on Text   Date: 05.06.2024, 14:01:01
I don't think the temporal resolution has been mentioned before... this should be said in 2.1.2.

Number: 11   Author: anonymous   Subject: Cross-Out   Date: 05.06.2024, 14:01:01

Number: 12   Author: anonymous   Subject: Comment on Text   Date: 05.06.2024, 14:01:01
This should go when the architecture is first mentioned

Number: 13   Author: anonymous   Subject: Cross-Out   Date: 05.06.2024, 14:01:01

Number: 14   Author: anonymous   Subject: Cross-Out   Date: 05.06.2024, 14:01:01

Number: 15   Author: anonymous   Subject: Cross-Out   Date: 05.06.2024, 14:01:01

Number: 16   Author: anonymous   Subject: Cross-Out   Date: 05.06.2024, 14:01:01

Number: 17   Author: anonymous   Subject: Cross-Out   Date: 05.06.2024, 14:01:01

Number: 18   Author: anonymous   Subject: Cross-Out   Date: 05.06.2024, 14:01:01
provides

Number: 19   Author: anonymous   Subject: Cross-Out   Date: 05.06.2024, 14:01:01
with the

Number: 20   Author: anonymous   Subject: Cross-Out   Date: 05.06.2024, 14:01:01

Number: 21   Author: anonymous   Subject: Highlight   Date: 05.06.2024, 14:01:01
unclear what that is, which primary?

Number: 22   Author: anonymous   Subject: Cross-Out   Date: 05.06.2024, 14:01:01

Number: 23   Author: anonymous   Subject: Highlight   Date: 05.06.2024, 14:01:01
again what does that mean?

Number: 24   Author: anonymous   Subject: Comment on Text   Date: 05.06.2024, 14:01:01
This is missing the information that ResBlocks are skip connections. This should be mentioned otherwise we don't understand where the input from earlier layers comes from.

2.1.3 Constraint layers

We test the CNN with three different constraining methods in the last CNN layer: 1- soft constraining (SCL), 2- hard constraining (HCL) and 3- without constraining (NoCL). ~~For a detailed information on the settings used we refer to the work of Harder et al. (2023). In the following, we explain briefly the three different constraining methodologies.~~ The set-up of constraining is as following: consider a factor N for downscaling in all linear directions and let $n := N^2$ and y_i, $i = 1, ..., n$ be the high-resolution patch values that correspond to low-resolution pixel x. The mass conservation law has the following form:

$$\frac{1}{n} \sum_{i=1}^{n} y_i = x. \tag{1}$$

Hard constraining: ~~It~~ uses ~~the~~ SoftMax ~~constraining, which is a constraining~~ for quantities like water content. ~~It enforces~~ the output to be non-negative. ~~For constraining the predicted quantities, we use a~~ SoftMax operator on the intermediate outputs of the ~~neural networks~~ before the constraining layer ($\tilde{y}_i$) and multiply ~~it~~ with the corresponding input pixel value x:

$$y_i = \exp(\tilde{y}_j) \cdot \frac{x}{\frac{1}{n} \sum_{i=1}^{n} \exp(\tilde{y}_i)}. \tag{2}$$

y_i is the final output after applying the constraints. We have used the mean absolute error (MAE) as the loss function.

Soft constraining: This is done by adding a regularization term to the loss function. The MAE loss then extended with an additional constraint violation (CV) loss term

$$\text{Loss} = (1 - \alpha) \cdot MAE + \alpha \cdot \text{CV}, \tag{3}$$

where CV ~~is the constraint violation, which~~ is the mean-squared error over all constraint violations between an input pixel x ~~and~~ the super-pixel (high-resolution grid-cell) y_i:

$$\text{CV} = \text{MSE}(\frac{1}{n} \sum_{i=1}^{n} y_i, x) \tag{4}$$

We use ~~the~~ $\alpha = 0.99$ ~~in this study~~.

Without constraining: In this setup we remove the constraining layer after the last convolutional layer in the CNN.

The constraint layers are applied at the end of the CNN architecture, and all satisfy the criteria that the resulting high-resolution patch conserves the values in low-resolution pixels. The performance of the different settings is assessed through the MAE.

We use the mean absolute error (MAE) as the loss function. We use 160 epochs, with a batch size of 64 and a learning rate of 0.001 for training with HCL and NoCL; and 0.00001 for SCL. Training takes 15 hours on an NVIDIA Corporation Graphics

Page: 7

Ampere 104 [GeForce Ray Tracing Texel eXtreme (RTX) 3060 Ti Lite Hash Rate] graphics processing unit (GPU). We use

205   the same model set-up as in Harder et al. (2023), and the computational cost of the CNN is very high, therefore, we did not conduct any cross-validation in this study.

We must note that the MAE can be used as both a loss function and an evaluation metric. A loss function is used during training to optimize the neural network parameters, while an evaluation metric is calculated on the validation or test data set to evaluate the model on an independent dataset. Those are two different use cases, but both can use an MAE.

210   **2.2   Evaluation and testing**

According to Ciarlo et al. (2021), the choice of observational data significantly influences the added value calculation of an RCM, as well as the extreme events detection. To reduce these issues, they recommended to use observations with a resolution comparable to the one of the model. Therefore, for assessing the added value of CCLM with respect to the driving GCM, we use the Climate Hazards Group InfraRed Precipitation with Station data (CHIRPS) as our gridded observation. CHIRPS

215   has a resolution of 0.05° and covers the area between 50°S-50°N. CHIRPS is based on satellite information and station data, and, in contrast to reanalysis data, it is independent of climate model simulations. Therefore, CHIRPS could be an excellent alternative to similar but not identical coarse datasets like Global Precipitation Climatology Centre (GPCC) (Becker et al., 2013) for data-sparse regions with convective rainfall (Funk et al., 2015).

For testing the CNN methods, instead of CHIRPS, we use the corresponding CCLM simulation (20% of the data, as men-

220   tioned above) as our target. We calculate the metrics on the CNN and interpolated GCM outputs with respect to CCLM output.

The selected GCM, RCM and observational data are interpolated onto the RCM grid using the distance-weighted average method. Interpolation of the coarser grid to a higher resolution might create unrealistic values. This issue was discussed in the work of Ciarlo et al. (2021). Usually, the interpolation does not account for the physical processes and constraints that govern the original data, the statistical properties (like mean, variance and skewness) are not preserved, and it introduces artefacts

225   and errors that depend on the choice of interpolation method, the spatial distribution of the data points and the resolution ratio. Therefore, dynamical/statistical downscaling is used to increase the resolution of the climate data, and we use simple interpolation as a baseline in our study.

Since precipitation does not follow a normal distribution, following Hodson (2022), we use the MAE to explore the bias of the emulated and dynamically downscaled precipitation (F) against observations(O):

230   $$\text{MAE} = \frac{1}{T} \sum_{t=1}^{T} |F_t - O_t| \quad (5)$$

where T is equal to the number of time steps. We quantify the added value (AV) as the ability of the downscaling approach to decrease the MAE of the driving GCM when calculated against the reference dataset (CHIRPS or target CCLM simulation), i.e.:

This page contains no comments

$$AV = \mathrm{MAE}_{GCM} - \mathrm{MAE}_{CCLM} \tag{6}$$

235 where MAE_{GCM} and MAE_{CCLM} are the differences of interpolated GCM and RCM with respect to the reference dataset.

As an additional metric we also use the climatological bias, i.e., the difference between the model and observations:

$$\mathrm{BIAS} = \mathrm{PR}_{MODEL} - \mathrm{PR}_{OBS} \tag{7}$$

3 Results

Figure 3.a shows the topography of the CORDEX-CA simulation domain. Figure 1.b presents the mean daily precipitation
240 averaged over all years (mm/day) as derived from CHIRPS data for the period 1985-2014. The regions with the highest values
of precipitation are the mountainous areas of CA. Additionally, also the Asian summer monsoon region north of India and
along the Himalayas in the southeastern part of the domain present pronounced precipitation values. Figure 3.c shows the
distribution of the WorldClim weather stations (Fick and Hijmans, 2017) over CA, representing a proxy for the density of the
station data used in the CHIRPS dataset. Over East China, especially over the Tibetan Plateau, the observation data distribution
245 is sparse. The data-model comparison is considered unreliable over this region (Randall et al., 2007; Cui et al., 2021; Yan et al.,
2020; Russo et al., 2019).

3.1 Added value of CCLM driven by ERAInterim

To characterize the overall performance of the CCLM model in time and space, Figures 4 and 5 show the maps of annual,
winter (DJF), and summer (JJA) MAE and mean biases of precipitation between interpolated ERAInterim and CCLM driven
250 by ERAInterim, calculated over the period 1985-2014 with respect to CHIRPS (Eq. 5 and Eq. 6). Figures 4.a-c show the
MAE of ERAInterim with respect to CHIRPS for annual, winter and summer averages. The added value of the CCLM RCM
compared to the interpolated ERAInterim GCM are shown in Figures 4.d-f. CCLM's MAE is high during the Asian summer
monsoon, over the South and Southeast of the domain (regions in magenta). During winter, the MAE is generally lower. CCLM
presents a MAE reduction for mountainous areas of Afghanistan, Kyrgizstan and Tajikistan and an increase of MAE near the
255 boundaries: South of the domain throughout the year, South and Southeast during the summer.

Added values of GERICS-REMO2015 and RMIB-UGent-ALARO-0 driven by ERAInterim are shown in Figure 4.g-l re-
spectively. The CHIRPS dataset is again used as the observational dataset O. The added value of RCM is the most pronounced
over areas with complex topography and especially during summer, for all three RCMS considered (Figs.4.d-l). Areas where
the RCM has smaller MAE than the reanalysis with respect to observations are located over Tajikistan, Kyrgyzstan, North of
260 Afghanistan and part of the Himalayas. Mountain areas of Tajikistan and Kyrgyzstan are the main source of water for the former
Soviet Union countries. However, precipitation during the colder seasons might be of more importance for water availability.

This page contains no comments

The annual AV patterns still show positive values over those areas (Figure 4.d,g and j). Considering the whole domain, all three RCMs sensibly reduce the large and local-scale bias of ERAInterim against CHIRPS, especially for complex topographies. The nested RCMs show similar values of MAE near their lateral boundaries, with respect to their driving model (Figure 4, *a*,*b*,*c*). Therefore, negative AV quantities might originate from the boundary effect, especially near the east and southeastern boundaries, where the monsoonal precipitation is dominant. GERICS-REMO2015 shows pronounced negative added values for annual and winter above Tibet.

As an additional check, we also show the bias in the climatologies of models in figures 5. Once again the biases are pronounced on the right bottom corner of the domain during the JJA and south Tibetan Plateau throughout the year.

3.1.1 Extreme precipitation patterns in CCLM and CMIP6 GCMs

Given that the CCLM simulation has shown some added value for precipitation over mountainous areas of CA, we explore climate change signals in its high-resolution output. The resulting high-resolution maps might have biases inherited from the GCM-RCM selection. We assume that many model biases remain conserved among the different time slices and, therefore, can be removed when calculating the changes between the historical (1985-2014) and future periods (2070-2099).

We present the resulting climate change trends in CCLM and the CMIP6 GCMs ensemble statistics (ensemble mean and standard deviation). We analyzed 31, 33 and 38 models for SSP126, SSP370 and SSP585 scenarios with a total number of simulations of 158, 185 and 242, respectively (see Supplementary materials for the list of models used in this study). To give the same weight to individual models, we first calculate the statistics over all the members of each model and then build the final statistics. We have chosen the yearly 99th percentile of daily precipitation (PR99 hereafter), which considers the three days of the year with the highest precipitation. We also chose the number of very heavy precipitation days in the period (ECA_RX20mm) as a different index, one of several precipitation-related indices used to monitor and analyze climate variability and change. For example, this index is often used in climate research to assess the impacts of very heavy precipitation events on water resources, agriculture, and natural ecosystems (Klok and Klein Tank, 2008). Figure 6 presents the changes in averaged PR99 at the end of the century (2070-2099) with respect to the historical period (1985-2014) for CCLM (a,d and g) and CMIP6 GCMs (b,e and h) under different scenarios. The downscaling signals indicate that those characteristics depend on the scenario and time period. The large-scale patterns remain the same among all three selected scenarios with intensification when the anthropogenic influence increases. The standard deviation of the models' ensemble is shown in Figures 6.c,f and i. According to our analysis, the Himalayas, especially Nepal, North India, and Bhutan, have the highest uncertainty among the GCMs and in all scenarios. Except for this area and the eastern boundary of the domain, the standard deviation remains under 3 mm/day. Under the pessimistic SSP585 and the regional rivalry SSP370 scenarios, areas with more than 9 mm/day increase in PR99 for CCLM over Northwest India, North Pakistan, North Iran, Southwest of Iran exist and South and Southeast of Black Sea. A reduction pattern is detected East of the Mediterranean Sea in Jordan, Syria, and South of Turkey. Similar patterns are also observed in the CMIP6 ensemble mean. However, due to the averaging, the GCMs' ensemble mean patterns are around $\pm$ 5 mm/day over those areas. Under the SSP126 scenario, which agrees with the 2°C target, the increasing patterns of more than $\pm$ 9 mm/day for CCLM and $\pm$ 5 mm/day for GCMs disappeared. In CA, areas of increased PR99 over Kyrgyzstan, Tajikistan,

This page contains no comments

North of Pakistan and Southwest Iran are regions with a considerable risk of rainfall-triggered events like landslides (Wang et al., 2021; Kirschbaum et al., 2010) and floods (for example, Pakistan floods of 2010 and 2022).

Figures 7.1,d and g show the ECA_RX20mm values for CCLM for the three scenarios at the end of the century. The patterns are like those shown in Figure 6, indicating that the number (frequency) of very heavy precipitation days also increases with an enhanced anthropogenic influence, particularly over the Tibetan Plateau. From Figures 7.b,e and h, we conclude that the CMIP6 GCM ensemble also presents a very similar behavior to CCLM. The ensemble standard deviations, however, increase over Tajikistan and Kyrgyzstan for ECA_RX20mm values (Figures 7.c,f and i). The increased frequency and intensity of extreme precipitation over elevated areas of CA due to anthropogenic forcing is alerting (Fallah et al., 2023). The presented CCLM simulation contributes to study the sensitivity of dynamical downscaling to different levels of anthropogenic forcing at the local scale. This information might be of interest for the scientific community working on the impact of climate change in CA.

4   CCLM emulator using a CNN

We have shown that the dynamical downscaling added value to explore the local effects of climate change during the historical period, especially over areas with enhanced topographical forcings. Here, we create an emulator of CCLM for precipitation over CA. As explained previously, a CNN could be trained on our GCM-RCM chain and be applied as a fast and computationally cheap downscaling method. However, the skill of such a model must be explored and verified.

Here we want to demonstrate that the emulator is better at downscaling than a simple interpolation, especially for areas receiving extreme precipitation values. More specifically, our goal is to show that the CCLM emulator can produce CCLM-like patterns when fed by the parent GCM.

For the CNN approach, we focus on the CA domain covering only the former Soviet Union countries (Kazakhstan, Kyrgyzstan, Tajikistan, Turkmenistan, and Uzbekistan) and not the CORDEX-CA domain previously shown in Figure 3. This domain is the region of interest in the Green Central Asia project https://www.greencentralasia.org/en, which is financed by the German Foreign office. Figure 8.a shows the MAE of the interpolated MPI-ESM1-2-HR using the CCLM driven by it from the test dataset as the "true" precipitation. As can be seen, CCLM produces different precipitation values compared to its driving GCM, especially over regions with complex topography. Here, we assume that the CCLM is the ground truth and check if the CNN can produce it using the GCM as input data. To evaluate the performance of the emulator, we show the maps of added value in Figures 8.b-d. Comparison of MAE reduction maps shows that the unconstrained CNN produces significant skills over elevated regions of CA and the constrained runs do not present considrable patterns of changes. For example, there are areas of negative and positive added values remarkably close together over elevated areas of CA created by HCL and SCL emulators. NoCL, in contrast, shows systematic positive values over large parts of the domain. There are several artifacts in the MAE reduction maps of constrained models, especially over North of India, which represent the GCM grid shape. We produce the boxplots of daily precipitation over the CA domain covering the former soviet union to explore the improvement in the distributions (Figure 9). The correlation coefficients between the time-series of average precipitation over the domain

This page contains no comments

with respect to CCLM are also presented in Figure 9 (values in the parentheses). For the daily averages, NoCL presents the best
330 performance (highest correlation coefficient). However, the values of outliers are smaller than the ones from CCLM and all
other model simulations. The distribution is more condensed around the median (smallest interquartile range). The distribution
of both constrained models (HCL, SCL) is like the interpolated GCM one. This was expected, since the constraining conserves
the mass of high-resolution grid-boxes within the corresponding low-resolution grid-box (Equation 1).

4.1 Applying the CNN to a different GCM

335 We evaluate the emulator's generalization ability, i.e. the ability to create reliable predictions on a new data set. We conduct a
new 15-year dynamical simulation with CCLM driven by the EC-Earth3-Veg (Döscher et al., 2022) GCM under ssp370 from
2019 to 2033. We use this data as input to our CCLM emulator, which was previously trained to emulate CCLM using MPI-
ESMI-2 HR as input GCM. We now use the emulator to reconstruct the local features of CCLM driven by EC-Earth3-Veg.
Figure 10.a presents the MAE of the interpolated EC-Earth3-Veg with respect to the dynamical downscaling with CCLM,
340 i.e., the CCLM simulation driven by EC-Earth3-Veg. The MAE pattern of EC-Earth3-Veg is remarkably like the one from
MPI-ESM1-2-HR (Figure 8.a). However, the CCLM emulator based on the NoCL CNN model does not show positive error
reduction everywhere in the domain (Figure 10.b). We chose the NoCL CNN because it showed the best performance among the
constrained ones. Training the CNN on the MPI-ESM1-2-HR/CCLM might have ignored learning processes which overcome
considerable biases in the driving GCM. The CCLM emulator tries to find relations between the MPI-ESM1-2-HR and CCLM,
345 which might be specific to these two models and there is no guarantee that those relationships also apply to the new EC-Earth3-
Veg and CCLM driven by EC-Earth3-Veg. This new GCM-RCM chain is extremely sensitive to the characteristics of the EC-
Earth3-Veg model because, as we showed previously, the RCM state follows the state of its driving GCM. We note that CCLM
is driven at the lateral boundaries by the GCM values for the state variables of CCLM (temperature, pressure, wind speed etc.).
Precipitation is not used for driving the RCM. The CNN input is the GCM precipitation, which has different biases in the two
350 GCM, and therefore the mapping from the MPI-ESM1-2-HR-precipitation to the CCLM precipitation cannot be successfully
transferred to EC-Earth3-Veg.

Knowing these limitations, the CNN model shows added values of more than 1 mm/day over the Alborz Mountains and South
of the Caspian Sea in the North of Iran (black rectangular in Figures 10.a and b) and some parts of Tajikistan and Kyrgyzstan.
Exploring the field mean of daily precipitation distribution indicates that the CNN's median value and the outliers are lower
355 than both the EC-Earth3-Veg and CCLM simulations (Figure 10.c). Only the day-to-day correlation is being improved. As
mentioned before, all model were trained on the shuffled dataset and ignored the memory in the time series but here the trained
NoCL model was given unshuffled EC-EARTH3-Veg to make new predictions. The correlation coefficient increases using the
NoCL model from 0.815 (EC-Earth3-Veg) to 0.844 (NoCL). Over the black rectangular box in Figure 10.b, the region where
the NonCL model reduces the MAE, i.e., the distribution of precipitation converges to the one from CCLM (Figure 10.d)
360 and receives the highest amount of precipitation in Iran and supplies water for a large portion of population in the country,
including the capital city Tehran with a population of over 10 million people. Only the outliers larger than 20 mm/day are not
reconstructed by the NoCL.

This page contains no comments

As a new test for generalization, we intentionally did not include a scenario (SSP370) in the training process. This move allowed us to apply the model to a specific simulation and witness its ability to reproduce an unknown forcing. Figure 11

365 demonstrates the AV of the CNN emulator for SSP370 in comparison to the dynamical downscaling with CCLM, i.e., the CCLM simulation driven by SSP370. The AV pattern is strikingly similar to the one shown in Figure 8.d. We conclude that the CNN can learn patterns it was not trained for, as evidenced by the SSP370 scenario.

5   Discussion and conclusions

Regional climate change impact assessments require high resolution climate projections. The main strategies to produce such

370 datasets are statistical and dynamical downscaling, as well as a hybrid of the two methods. Statistical downscaling (SD) usually has limited capability to consider the dynamic influences of the complex topography. The large-scale domain does not reflect the spatial diversity and variation of the local climate and the topography, which may affect the accuracy of the statistical relationships (Li et al., 2022). For SD applied to precipitation, the observations need to contain detailed information about the precipitation distribution in areas with complex topography (Lundquist et al., 2019). On the other hand, dynamical downscaling

375 requires massive computational time and data storage space. A 30-year CCLM simulation driven by ERAInterim took roughly one week to finish using 216 processors of the HLRE-4 Levante computer at the German Climate Computing Center (DKRZ). Additionally, the added value of RCMs is still debated since they are highly dependent on the driving GCMs.

In this study, we contribute to the few dynamical downscaling efforts over the CORDEX-CA domain, a small step towards an RCM ensemble creation for CA. A single RCM simulation can help identify model biases and uncertainties that need to be

380 addressed in future model improvements. It is essential to note that relying solely on a single model run for CMIP6 instead, of an RCM ensemble, may not provide any comprehensive understanding of the potential climate change impacts on a region. Therefore, it is recommended that researchers conduct multiple simulations with different initial and boundary conditions and different model configurations to account for the uncertainty associated with climate projections.

In a first part of the study we demonstrate the added value of RCMs (here we chose to use the COSMO-CLM/CCLM model)

385 over GCMs for CA in the representation of precipitation. Our CCLM run shows added value with respect to its driving GCM, comparable to the range of values obtained for other RCMs applied to the CORDEX-CA domain over the evaluation period. It also reproduces extreme precipitation changing patterns like the CMIP6 ensemble mean at the end of the century. Both CCLM and CMIP6 ensemble present elevated risk (frequency and intensity) of heavy precipitation events over vulnerable areas of CA due to different anthropogenic influences.

390 Our study evaluated the downscaling skill primarily using higher resolution observations, which are critical for capturing localized climate phenomena relevant to regional adaptation strategies. However, as Volosciuk et al. (2017) noted, examining downscaling outputs at coarser resolutions can be equally informative. Their work emphasizes that downscaling methods can introduce or fail to correct biases that differ significantly across spatial scales. By evaluating on a coarser grid, it is possible to distinguish between the inherent biases of the model and those introduced by the downscaling process. This distinction

This page contains no comments

395 is crucial for understanding the limitations and strengths of downscaling methods in representing climatic variables across different scales.

Additionally, acknowledging the computational and memory constraints of running an RCM at high resolution, here we also show that a single GCM-RCM model chain can be used to train a climate emulator based on a CNN model. It can learn some nonlinear and physical relationships between the coarse and fine-resolution datasets. This can overcome the problem of spatial
400 intermittency seen in some statistical downscaling approaches (Harder et al., 2023). However, we have also shown that the CNN model has limitations, namely when generalizing, as it did not achieve a robust error-reduction pattern given a different GCM as input. The learning process depends strongly on the GCM/CCLM relationships. More importantly, an RCM is forced to follow its driving GCM and only on local scales can produce extra information. An application of the presented CCN could be to apply it for other experiments of the same GCM: One could use the trained emulator for paleo-climate experiment of
405 the parent GCM to create more than 10,000 years of downscaled simulation. One can also downscale the volcanic forcing experiments using the trained emulator. This will aid the paleo-climate community in conducting proxy-model comparisons at local scales. However, previous studies have shown that the CNN suffers from the same generalisation problem as when applied to a new GCM and such applications must be tested (Jouvet and Cordonnier, 2023).

In an effort to evaluate the model's generalization capabilities, we deliberately excluded the SSP370 scenario from the train-
410 ing dataset. This strategy was implemented to assess whether the model could effectively infer and replicate patterns from untrained scenarios. Remarkably, the model's output for the SSP370 scenario exhibits an AV pattern that closely mirrors the dynamical downscaling results obtained with the CCLM, driven by the same SSP370 scenario. This alignment strongly supports the notion that our CNN emulator is not only capable of learning from its training data but also proficient in generalizing to new, unseen conditions. The similarity in AV patterns between the model output and the CCLM simulation underscores the
415 robustness and adaptability of our model, affirming its potential for broader applicative scenarios in climate modelling.

We note that this work is only a step to demonstrate the potential of such a hybrid approach, and we encourage the community to explore different model structures and parameter combinations for further improvement. For example, our few model set-ups showed that using a physically constrained CNN set-up, that applies a linear transformation to the high-resolution image to ensure that the total mass or energy is conserved between the low and high-resolution images, did not successfully downscale
420 the precipitation. The constraints might not be satisfied in the original dataset and therefore the constrained model set-up did not lead to better results. In contrast, with a higher degree of freedom, the unconstrained CNN produced patterns closer to the target RCM. Alternative machine learning models, such as generative adversarial networks (GANs), which can generate more high-frequency patterns, might improve the downscaled pattern, and could be tested in future studies. An additional set-up might be to provide more information to the CNN by adding characteristics like surface height, vegetation, land-cover,
425 land-use, etc. as new channels within the input layer.

Code availability. The code for "Physics-Constrained Deep Learning for Climate Downscaling," is available on Zenodo at the following DOI: https://zenodo.org/uploads/8150694. The input, output, trained models, a snapshot of the code employed in the deep-learning down-

This page contains no comments
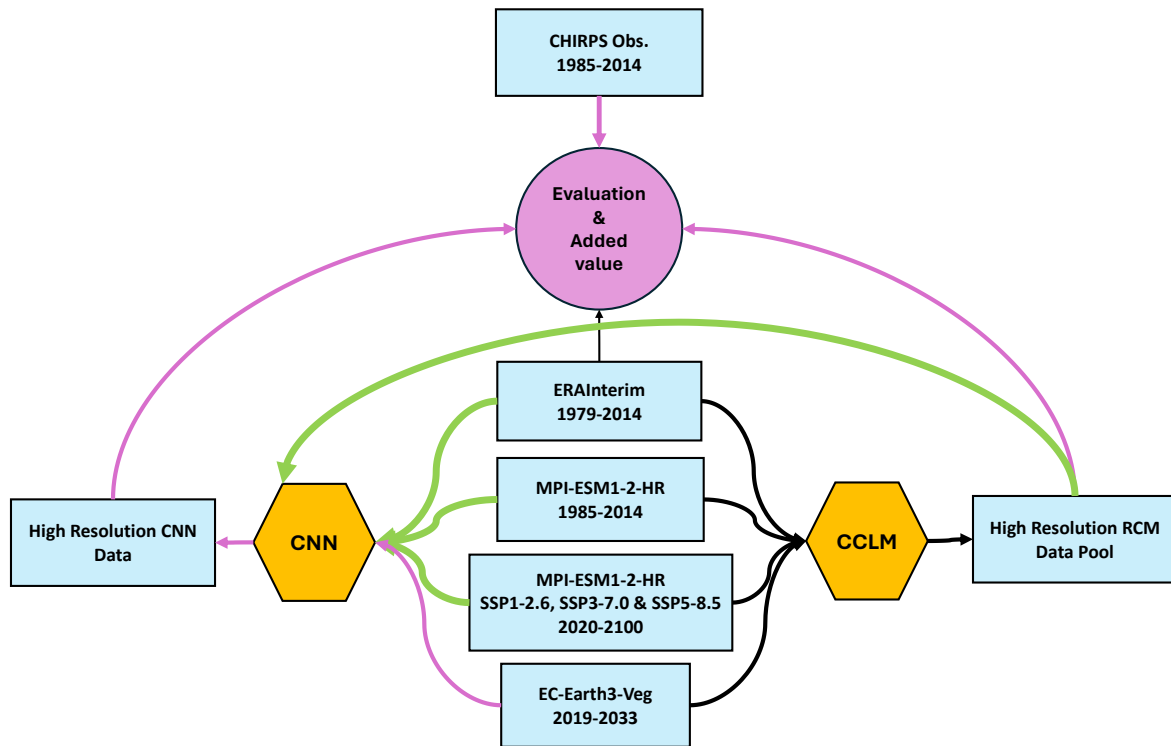
Figure 1. Schematic of the methodology used in this study. Green arrows show the data flow used for training the CNN and magenta for evaluation and calculation of the added values. Datasets are shown by rectangular, downscaling models by hexagonal and evaluation analysis by circle.

scaling process, COSMO-CLM model setups for all Regional Climate Model (RCM) simulations conducted, a list of CMIP6 model information used for comparative analysis, and a Jupyter notebook for executing a test case of the "Physics-Constrained Deep Learning for Climate

430 Downscaling" as described in the manuscript are available at Zenodo with the following DOI: https://zenodo.org/records/10417111.

Appendix A: CNN runs

We used the following commands for training the CNN model based on the Harder et al. (2023):

```
# for the run with soft constraining run, with a factor of alpha 0.99 :

435

$ python main.py --dataset dataset --model cnn --model_id
twc_cnn_soft_constraints_epochs_160_lr_0.00001_alpha_0.99
--constraints soft --loss mass_constraints --alpha 0.99
 --epochs 160 --batch_size 64 --lr 0.00001

440

# for the run with softmax constraining or hard constraining :
```

This page contains no comments
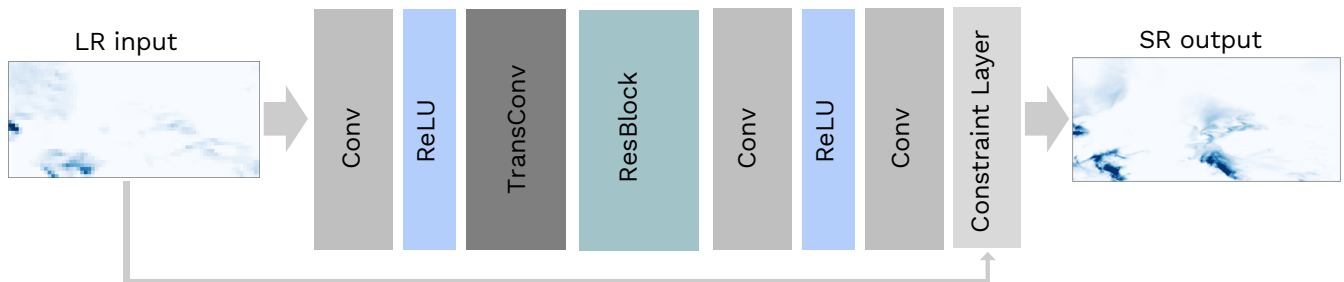
Figure 2. Schematic of the CNN architecture for 2 times upsampling with the constraints layer. The inputs are low-resolution (LR) images of size 30×60 and the output is a super-resolution (SR) image of size 60×120. This figure is modified from (Harder et al., 2023).

```
$ python main.py --dataset dataset --model cnn --model_id
twc_cnn_softmaxconstraints_epochs_200_batch_size_64_lr_0.001
--constraints softmax --lr 0.001 --epochs 160 --batch_size 64 --loss mae
```

445

```
# for the standard CNN run without constraining:
$ python main.py --dataset dataset --model cnn --model_id
twc_cnn_noneconstraints_epochs_160_batch_size_64_lr_0.001
```

450
```
--constraints none  --lr 0.001 --epochs 160 --batch_size 64 --loss mae
```

Note that the datasets and codes are available at Zenodo (DOI: https://zenodo.org/records/10417111) with comprehensive details utilized in the paper.

Author contributions. BF, conducted the dynamical and statistical downscaling with help of ER and PH, respectively. ER provided the CCLM set-up. PH provided the deep learning model code and set-up. All authors contributed to the analysis of the results and writing the
455 manuscript.

Competing interests. No competing interests.

This page contains no comments
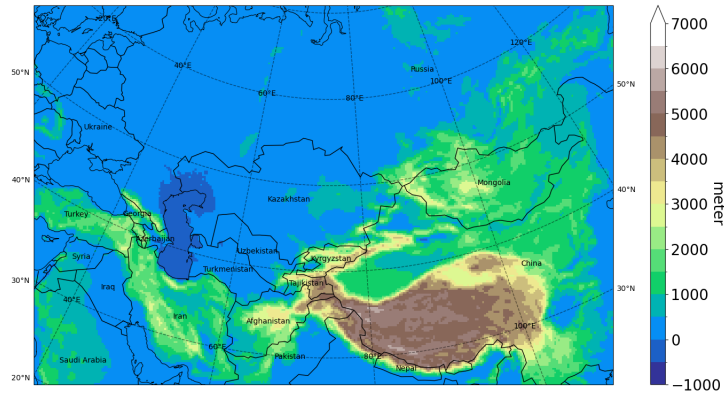
(a)
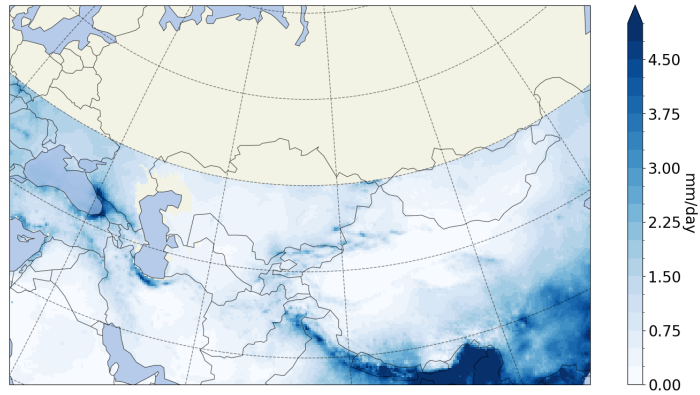
(b)
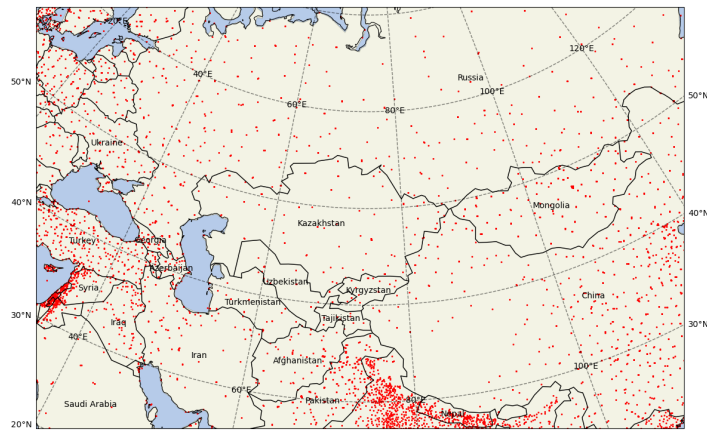
(c)

Figure 3. a) CCLM simulation domain over Central Asia and the topography (m), (b) CHIRPS climatology for 1985-2014 (average of daily values over all years in mm/day), and (c) WorldClim's weather stations (red dots).

This page contains no comments
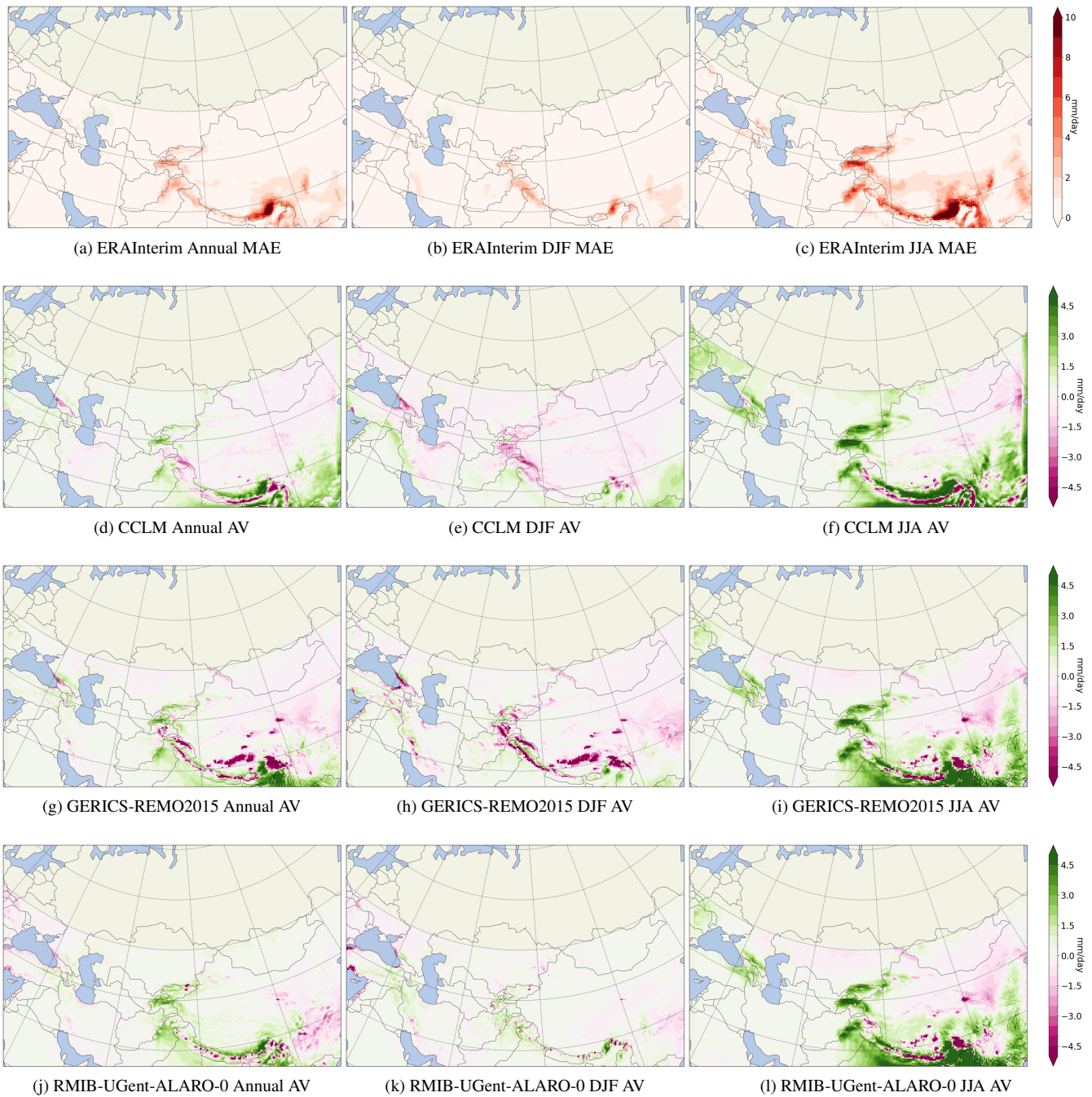
Figure 4. Mean average error (MAE) of daily precipitation (mm/day) from ERAInterim, as well as, added value (AV) as measured by MAE differences between ERAInterim and RCMs (MAE$_{\text{ERAInterim}}$ − MAE$_{\text{RCM}}$) in mm/day for annual (a,d,j,i), December, January, February (b,e,h,k) and June, July, August (c,f,i,l). CHIRPS is used as observation. All daatasets are interpolated to the CCLM grid.

This page contains no comments
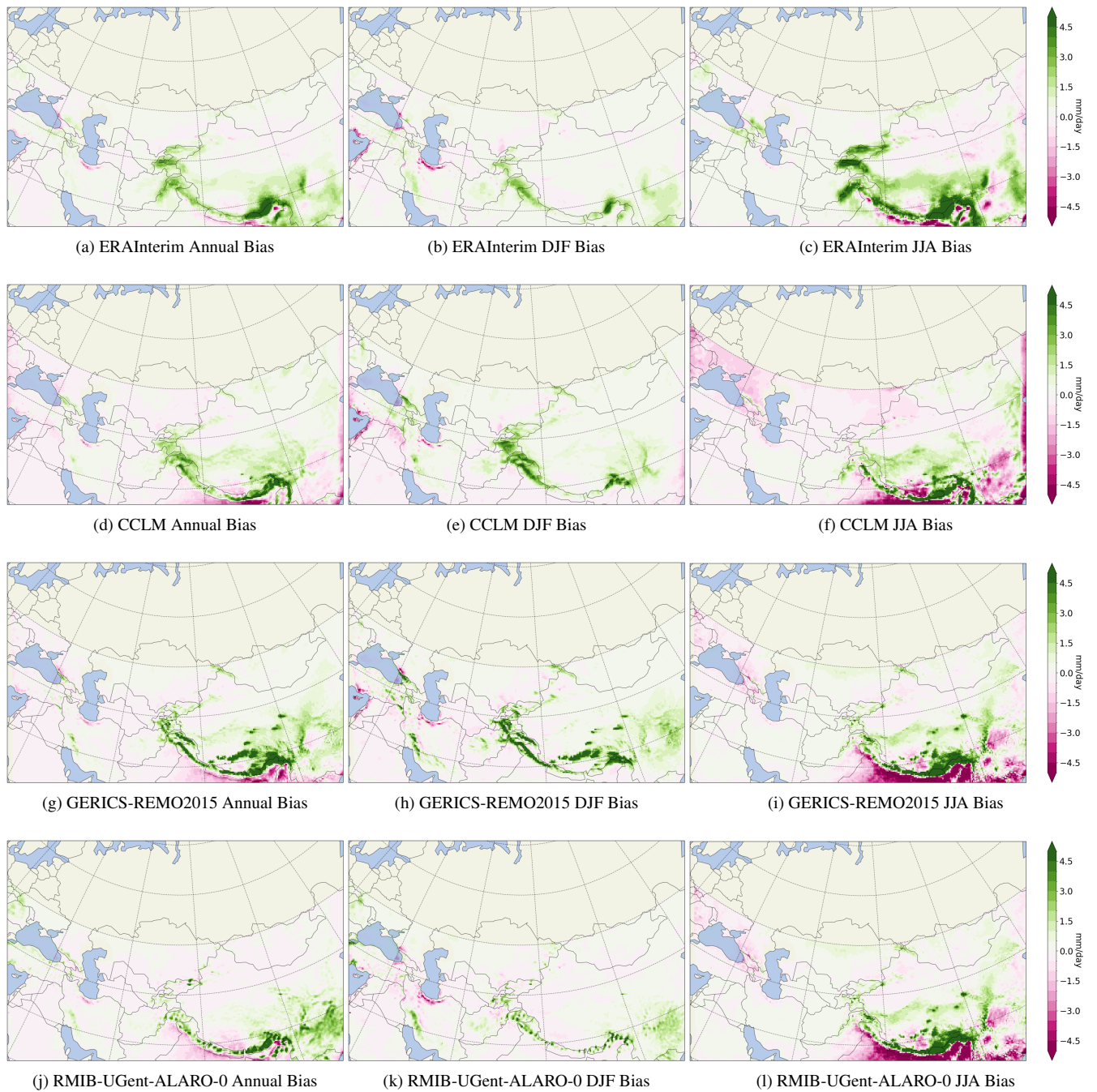
Figure 5. Bias of climatological precipitation (mm/day) from ERAInterim, as well as, ERAInterim-driven RCMs ($PR_{ERAInterim-CCLM} - PR_{OBS}$) in mm/day for annual (a,d,j,i), December, January, February (b,e,h,k) and June, July, August (c,f,i,l). CHIRPS is used as observation.

This page contains no comments

(a) SSP126-CCLM (b) SSP126-CMIP6-ensmean (c) SSP126-CMIP6-ensstd

(d) SSP370-CCLM (e) SSP370-CMIP6-ensmean (f) SSP370-CMIP6-ensstd

(g) SSP585-CCLM (h) SSP585-CMIP6-ensmean (i) SSP585-CMIP6-ensstd
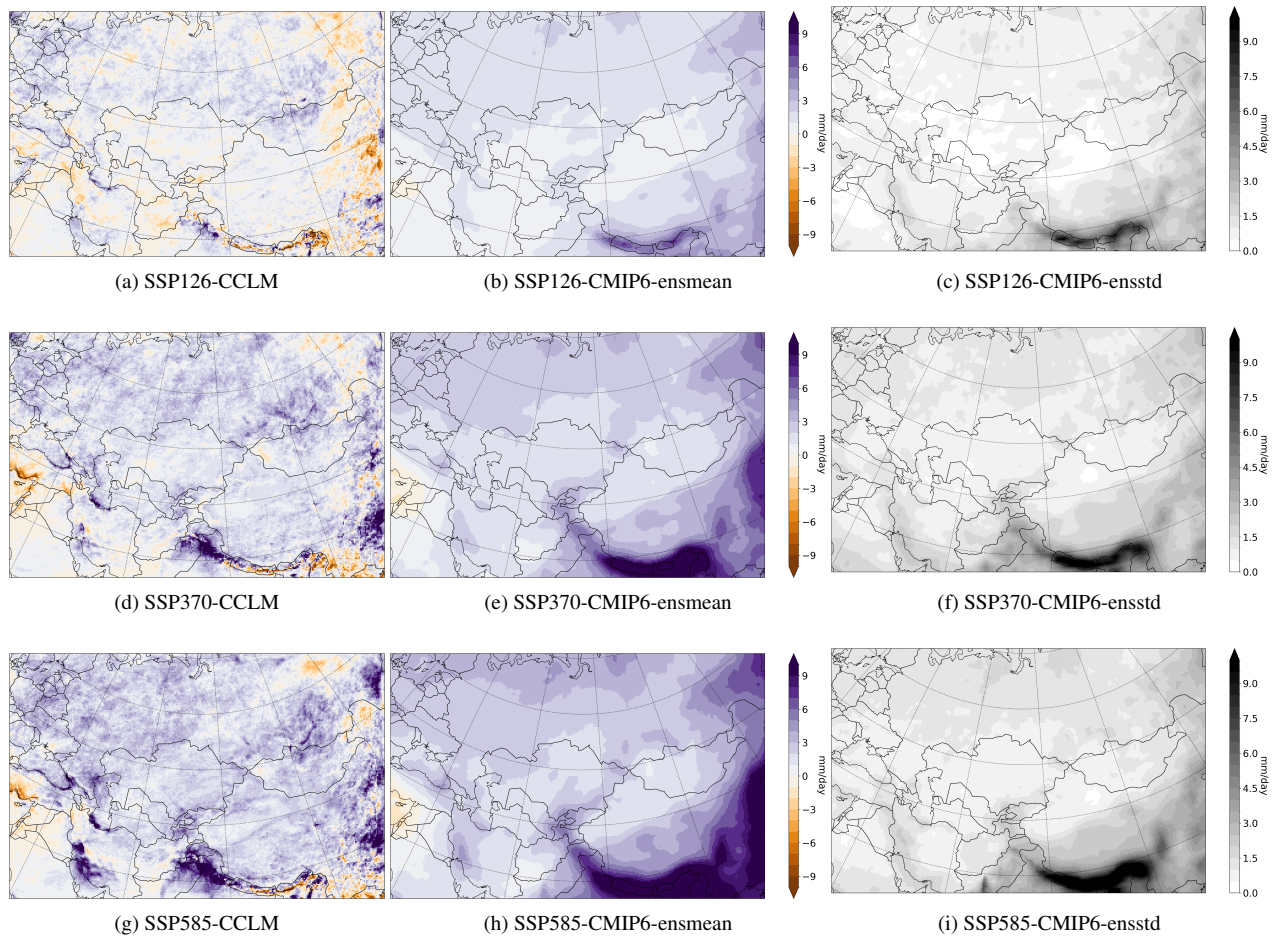
Figure 6. Changes in averaged yearly 99th percentile (3 days per year) of total precipitation (mm/day) with respect to 1985-2014 references for a,b) SSP126, d,e) SSP370 and g,h) SSP585 at the end of the century (2070-2099) from CCLM and CMIP6 GCMs' ensemble mean. The ensemble's standard deviations are shown in c,f and i.

Acknowledgements. BF thanks the German Climate Computing Center (DKRZ) for its support in using supercomputer data and resources. The German Foreign Office funds BF and ID via the Green Central Asia project (http://greencentralasia.org/en, last access: 4 July 2023). The DKRZ and PIK provided the computational resources. The authors gratefully acknowledge the German Federal Ministry of Education and Research and the Land Brandenburg for supporting this project by providing resources on the high performance computer system at the Potsdam Institute for Climate Impact Research. BF thanks the CCLM-community for providing the model code and the pre-processing code to convert the GCM to CCLM input files.

460

This page contains no comments
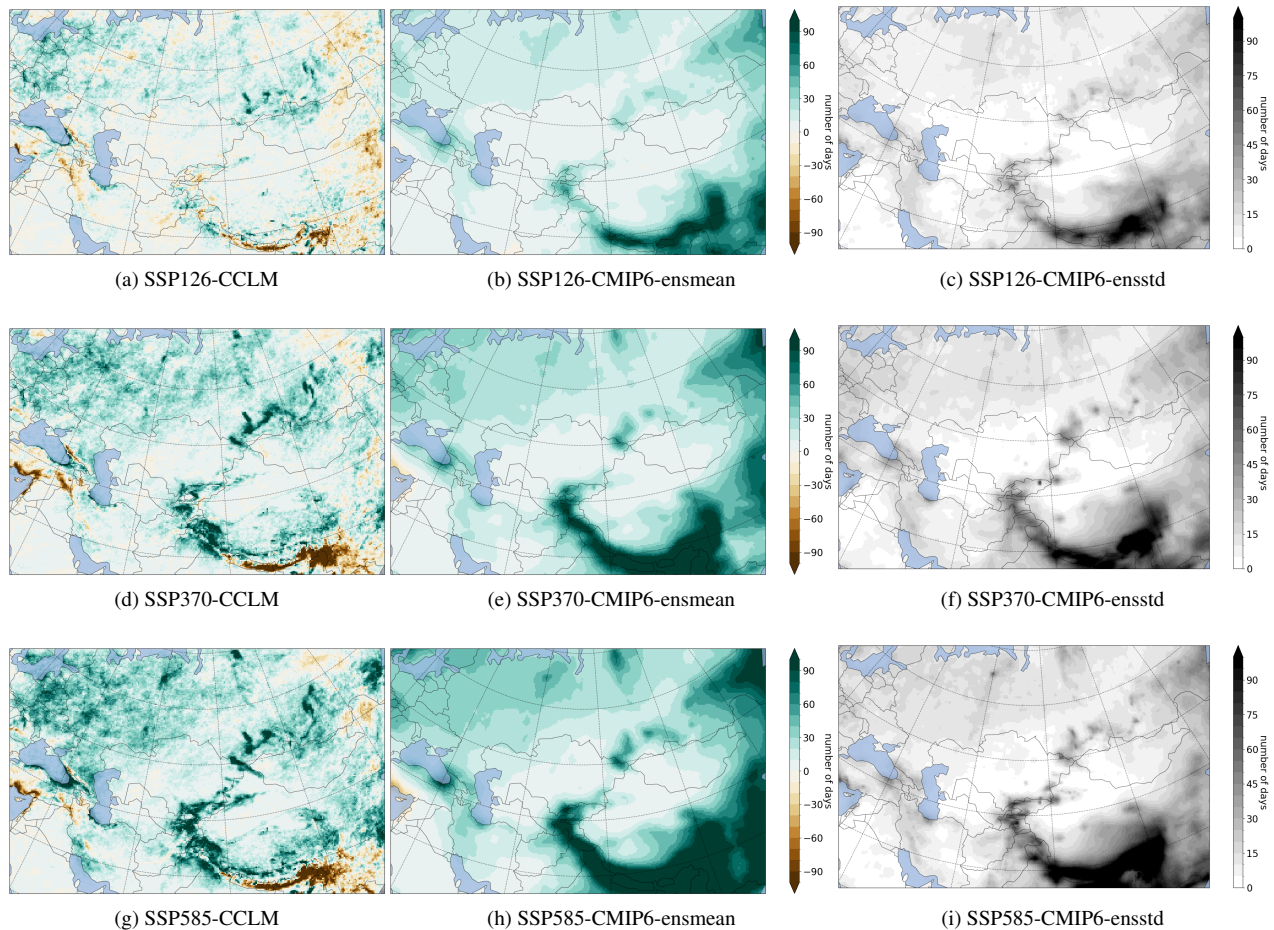
Figure 7. Changes in number of days with precipitation more than 20 mm in the period with respect to 1985-2014 references for a,b) SSP126, d,e) SSP370 and g,h) SSP585 at the end of the century (2070-2099) from CCLM and CMIP6 GCMs' ensemble mean. The ensemble's standard deviations are shown in c,f and i.

References

Allan, R. P., Hawkins, E., Bellouin, N., and Collins, B.: IPCC, 2021: summary for Policymakers, IPCC, 2021.

465   Ban, N., Schmidli, J., and Schär, C.: Heavy precipitation in a changing climate: Does short-term summer precipitation increase faster?, Geophysical Research Letters, 42, 1165–1172, 2015.

Becker, A., Finger, P., Meyer-Christoffer, A., Rudolf, B., Schamm, K., Schneider, U., and Ziese, M.: A description of the global land-surface precipitation data products of the Global Precipitation Climatology Centre with sample applications including centennial (trend) analysis from 1901–present, Earth System Science Data, 5, 71–99, 2013.

470   Böhm, U., Gerstengarbe, F.-W., Hauffe, D., Kücken, M., Österle, H., and Werner, P. C.: Dynamic regional climate modeling and sensitivity experiments for the northeast of Brazil, Global Change and Regional Impacts: Water Availability and Vulnerability of Ecosystems and Society in the Semiarid Northeast of Brazil, pp. 153–170, 2003.

This page contains no comments
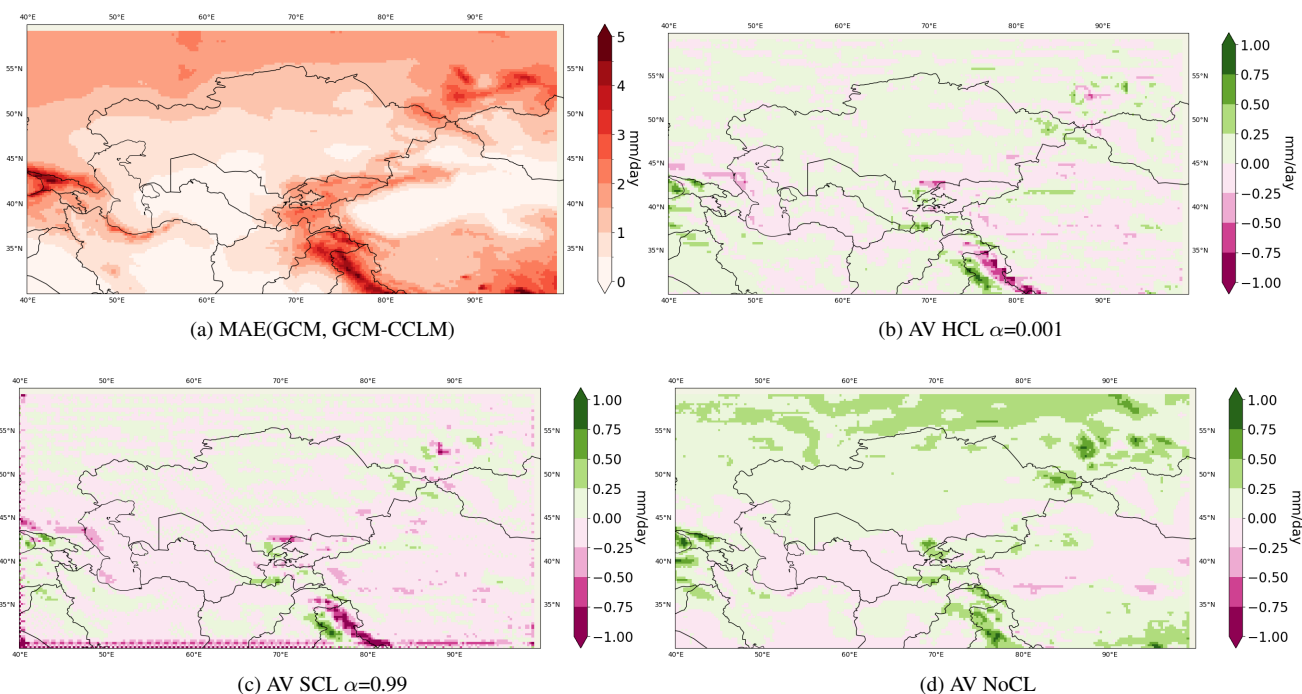
Figure 8. a) MAE (MPI-ESM1-2-HR,CCLM). MPI-ESM1-2-HR is remapped bilinearly to the 0.25×0.25 grid. b-d) Added Value (AV) or MAE(MPI-ESM1-2-HR,CCLM) - MAE(CNN,CCLM) for different constraining method.

Chokkavarapu, N. and Mandla, V. R.: Comparative study of GCMs, RCMs, downscaling and hydrological models: a review toward future climate change impact estimation, SN Applied Sciences, 1, 1698, 2019.

475 Ciarlo, J. M., Coppola, E., Fantini, A., Giorgi, F., Gao, X., Tong, Y., Glazer, R. H., Torres Alavez, J. A., Sines, T., Pichelli, E., et al.: A new spatially distributed added value index for regional climate models: the EURO-CORDEX and the CORDEX-CORE highest resolution ensembles, Climate Dynamics, 57, 1403–1424, 2021.

Cui, T., Li, C., and Tian, F.: Evaluation of temperature and precipitation simulations in CMIP6 models over the Tibetan Plateau, Earth and Space Science, 8, e2020EA001 620, 2021.

480 Demory, M.-E., Berthou, S., Fernández, J., Sørland, S. L., Brogli, R., Roberts, M. J., Beyerle, U., Seddon, J., Haarsma, R., Schär, C., et al.: European daily precipitation according to EURO-CORDEX regional climate models (RCMs) and high-resolution global climate models (GCMs) from the High-Resolution Model Intercomparison Project (HighResMIP), Geoscientific Model Development, 13, 5485–5506, 2020.

Di Luca, A., de Elía, R., and Laprise, R.: Potential for added value in precipitation simulated by high-resolution nested regional climate

485 models and observations, Climate dynamics, 38, 1229–1247, 2012.

Di Luca, A., de Elía, R., and Laprise, R.: Challenges in the quest for added value of regional climate dynamical downscaling, Current Climate Change Reports, 1, 10–21, 2015.

Didovets, I., Krysanova, V., Nurbatsina, A., Fallah, B., Krylova, V., Saparova, A., Niyazov, J., Kalashnikova, O., and Hattermann, F. F.: Attribution of current trends in streamflow to climate change for 12 Central Asian catchments, Climatic Change, 177, 16, 2024.

This page contains no comments
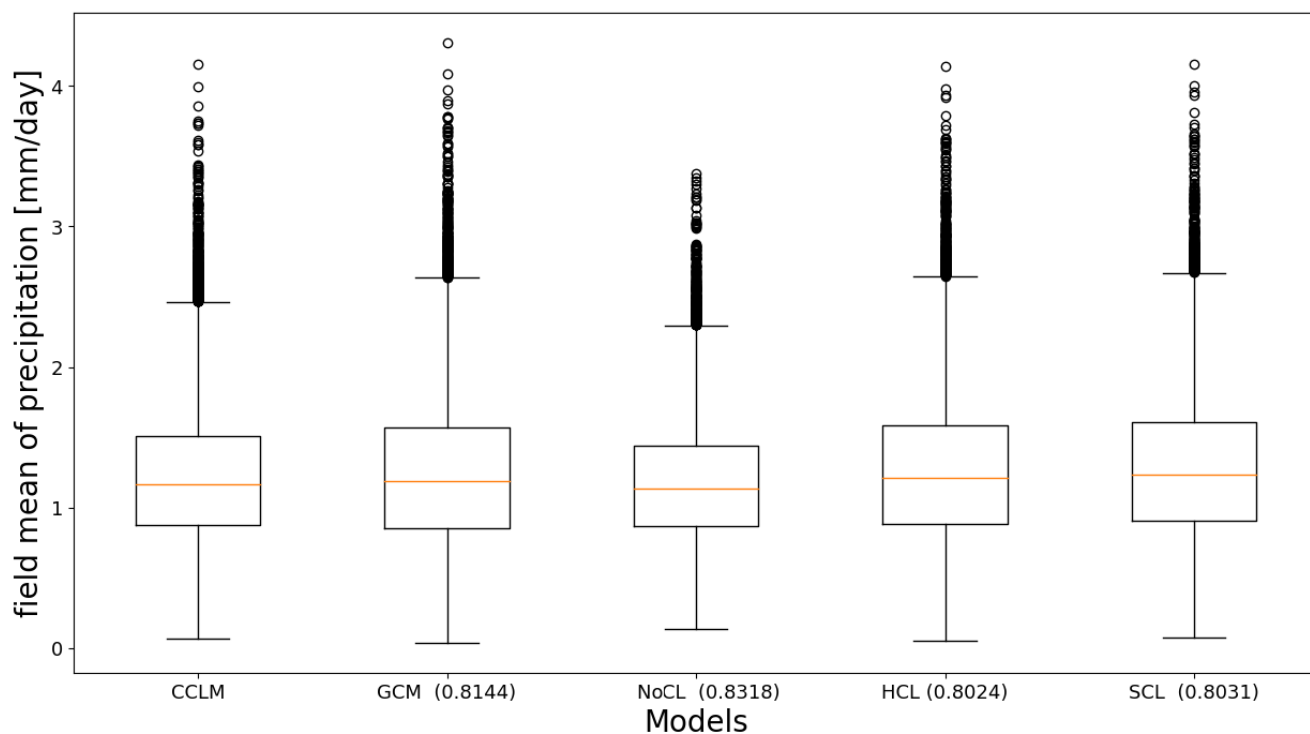
Figure 9. Boxplot of averaged daily precipitation over the Central Asian domain (shown in Figure 7) for different models and test dataset (22714 days or 62.2 years). Numbers in the parenthesis indicate the correlation coefficients between each model and the CCLM simulation.

490   Döscher, R., Acosta, M., Alessandri, A., Anthoni, P., Arneth, A., Arsouze, T., et al.: The EC-Earth3 Earth system model for the Coupled Model Intercomparison Project 6. Geosci. Model Dev. 15, 2973–3020, 2022.

Dosio, A. and Panitz, H.-J.: Climate change projections for CORDEX-Africa with COSMO-CLM regional climate model and differences with the driving global climate models, Climate Dynamics, 46, 1599–1625, 2016.

Fallah, B. and Rostami, M.: Exploring the impact of the recent global warming on extreme weather events in Central Asia using the counter-
495   factual climate data ATTRICI v1. 1, Climatic Change, preprint, https://doi.org/10.21203/rs.3.rs-2106031/v1, 2024.

Fallah, B., Saberi, A. A., and Sodoudi, S.: Emergence of global scaling behaviour in the coupled Earth-atmosphere interaction, Scientific Reports, 6, 34 005, 2016a.

Fallah, B., Sodoudi, S., and Cubasch, U.: Westerly jet stream and past millennium climate change in Arid Central Asia simulated by COSMO-CLM model, Theoretical and Applied Climatology, 124, 1079–1088, 2016b.

500   Fallah, B., Russo, E., Menz, C., Hoffmann, P., Didovets, I., and Hattermann, F. F.: Anthropogenic influence on extreme temperature and precipitation in Central Asia, Scientific Reports, 13, 6854, 2023.

Feser, F., Rockel, B., von Storch, H., Winterfeldt, J., and Zahn, M.: Regional climate models add value to global model data: a review and selected examples, Bulletin of the American Meteorological Society, 92, 1181–1192, 2011.

Fick, S. E. and Hijmans, R. J.: WorldClim 2: new 1-km spatial resolution climate surfaces for global land areas, International journal of
505   climatology, 37, 4302–4315, 2017.

This page contains no comments

(a) MAE(EC-Earth3-Veg, CCLM)

(b) AV NoCL

(c) CA
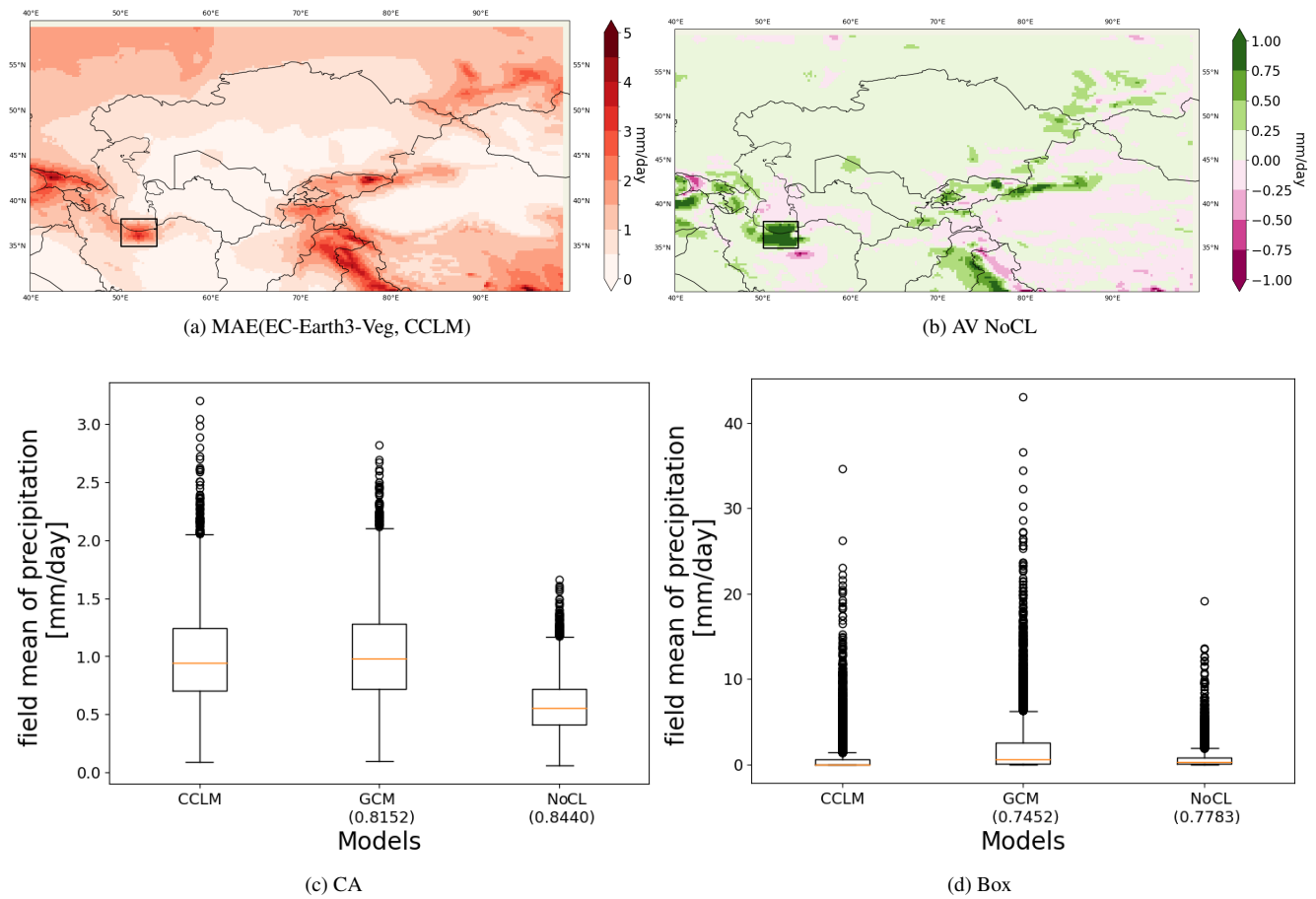
(d) Box

Figure 10. a) MAE of GCM (EC-Earth3-Veg) vs CCLM run. GCM is remapped bilinearly to the 0.25×0.25 grid. b) Added value (AV) or MAE reduction (MAE(EC-Earth3-Veg,CCLM) - MAE(CNN,CCLM) for unconstrained method. c) and d) boxplots of averaged daily precipitation over the CA domain and the black box shown in a and b over North of Iran. Numbers in the parenthesis indicate the correlation coefficients of each model with respect to CCLM.
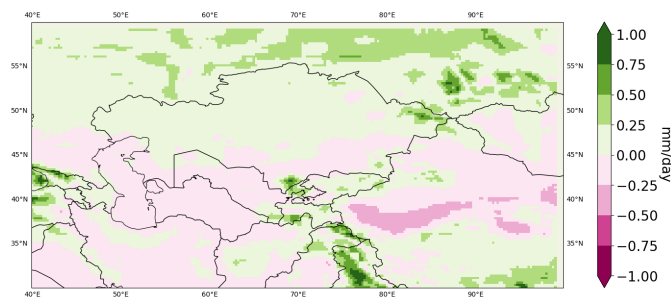
Figure 11. Added value (AV) or MAE reduction (MAE(EC-MPI-ESM1-2HR, CCLM)—MAE(CNN, CCLM)) for an unconstrained method that was not trained but applied to the SSP370 scenario.

This page contains no comments

Fotso-Nguemo, T. C., Vondou, D. A., Pokam, W. M., Djomou, Z. Y., Diallo, I., Haensler, A., Tchotchou, L. A. D., Kamsu-Tamo, P. H., Gaye, A. T., and Tchawoua, C.: On the added value of the regional climate model REMO in the assessment of climate change signal over Central Africa, Climate Dynamics, 49, 3813–3838, 2017.

Fowler, H. J., Blenkinsop, S., and Tebaldi, C.: Linking climate change modelling to impacts studies: recent advances in downscaling techniques for hydrological modelling, International Journal of Climatology: A Journal of the Royal Meteorological Society, 27, 1547–1578, 2007.

Frei, C., Christensen, J. H., Déqué, M., Jacob, D., Jones, R. G., and Vidale, P. L.: Daily precipitation statistics in regional climate models: Evaluation and intercomparison for the European Alps, Journal of Geophysical Research: Atmospheres, 108, 2003.

Funk, C., Peterson, P., Landsfeld, M., Pedreros, D., Verdin, J., Shukla, S., Husak, G., Rowland, J., Harrison, L., Hoell, A., et al.: The climate hazards infrared precipitation with stations—a new environmental record for monitoring extremes, Scientific data, 2, 1–21, 2015.

Galea, D., Ma, H.-Y., Wu, W.-Y., and Kobayashi, D.: Deep Learning Image Segmentation for Atmospheric Rivers, Artificial Intelligence for the Earth Systems, 3, 230 048, 2024.

Gardoll, S. and Boucher, O.: Classification of tropical cyclone containing images using a convolutional neural network: Performance and sensitivity to the learning dataset, Geoscientific Model Development, 15, 7051–7073, 2022.

Giot, O., Termonia, P., Degrauwe, D., De Troch, R., Caluwaerts, S., Smet, G., Berckmans, J., Deckmyn, A., De Cruz, L., De Meutter, P., et al.: Validation of the ALARO-0 model within the EURO-CORDEX framework, Geoscientific Model Development, 9, 1143–1152, 2016.

Harder, P., Hernandez-Garcia, A., Ramesh, V., Yang, Q., Sattegeri, P., Szwarcman, D., Watson, C., and Rolnick, D.: Hard-Constrained Deep Learning for Climate Downscaling, Journal of Machine Learning Research, 24, 1–40, 2023.

Hess, P., Drüke, M., Petri, S., Strnad, F. M., and Boers, N.: Physically constrained generative adversarial networks for improving precipitation fields from Earth system models, Nature Machine Intelligence, 4, 828–839, 2022.

Hodson, T. O.: Root-mean-square error (RMSE) or mean absolute error (MAE): When to use them or not, Geoscientific Model Development, 15, 5481–5487, 2022.

Jacob, D. and Podzun, R.: Sensitivity studies with the regional climate model REMO, Meteorology and atmospheric physics, 63, 119–129, 1997.

Jacob, D., Elizalde, A., Haensler, A., Hagemann, S., Kumar, P., Podzun, R., Rechid, D., Remedio, A. R., Saeed, F., Sieck, K., et al.: Assessing the transferability of the regional climate model REMO to different coordinated regional climate downscaling experiment (CORDEX) regions, Atmosphere, 3, 181–199, 2012.

Jacob, D., Petersen, J., Eggert, B., Alias, A., Christensen, O. B., Bouwer, L. M., Braun, A., Colette, A., Déqué, M., Georgievski, G., et al.: EURO-CORDEX: New high-resolution climate change projections for European impact research, Regional Environmental Change, 14, 563–578, 2014.

Jouvet, G. and Cordonnier, G.: Ice-flow model emulator based on physics-informed deep learning, Journal of Glaciology, pp. 1–15, 2023.

Kendon, E., Roberts, N., Fowler, H., Roberts, M., Chan, S., and Senior, C.: Heavier summer downpours with climate change revealed by weather forecast resolution model. Nat. Climate Change, 4, 570–576, 2014.

Kikstra, J. S., Nicholls, Z. R., Smith, C. J., Lewis, J., Lamboll, R. D., Byers, E., Sandstad, M., Meinshausen, M., Gidden, M. J., Rogelj, J., et al.: The IPCC Sixth Assessment Report WGIII climate assessment of mitigation pathways: from emissions to global temperatures, Geoscientific Model Development, 15, 9075–9109, 2022.

Kirschbaum, D. B., Adler, R., Hong, Y., Hill, S., and Lerner-Lam, A.: A global landslide catalog for hazard applications: method, results, and limitations, Natural Hazards, 52, 561–575, 2010.

This page contains no comments

Kjellström, E., Nikulin, G., Hansson, U., Strandberg, G., Ullerstig, A., Willén, U., and Wyser, K.: 21st century changes in the European climate: uncertainties derived from an ensemble of regional climate model simulations, Tellus A: Dynamic Meteorology and Oceanography, 63, 24–40, 2011.

Klok, E. and Klein Tank, A.: Updated and extended European dataset of daily weather observations, International Journal of Climatology, 28, 2081–2095, 2008.

Kotlarski, S., Keuler, K., Christensen, O. B., Colette, A., Déqué, M., Gobiet, A., Goergen, K., Jacob, D., Lüthi, D., Van Meijgaard, E., et al.: Regional climate modeling on European scales: a joint standard evaluation of the EURO-CORDEX RCM ensemble, Geoscientific Model Development, 7, 1297–1333, 2014.

Kurth, T., Treichler, S., Romero, J., Mudigonda, M., Luehr, N., Phillips, E., Mahesh, A., Matheson, M., Deslippe, J., Fatica, M., et al.: Exascale deep learning for climate analytics, in: SC18: International conference for high performance computing, networking, storage and analysis, pp. 649–660, IEEE, 2018.

Laflamme, E. M., Linder, E., and Pan, Y.: Statistical downscaling of regional climate model output to achieve projections of precipitation extremes, Weather and climate extremes, 12, 15–23, 2016.

Lenz, C.-J., Früh, B., and Adalatpanah, F. D.: Is there potential added value in COSMO–CLM forced by ERA reanalysis data?, Climate Dynamics, 49, 4061–4074, 2017.

Li, L., Bisht, G., and Leung, L. R.: Spatial heterogeneity effects on land surface modeling of water and energy partitioning, Geoscientific Model Development, 15, 5489–5510, 2022.

Lundquist, J., Hughes, M., Gutmann, E., and Kapnick, S.: Our skill in modeling mountain rain and snow is bypassing the skill of our observational networks, Bulletin of the American Meteorological Society, 100, 2473–2490, 2019.

Maraun, D. and Widmann, M.: Statistical downscaling and bias correction for climate research, Cambridge University Press, 2018.

Maraun, D., Widmann, M., Gutiérrez, J. M., Kotlarski, S., Chandler, R. E., Hertig, E., Wibig, J., Huth, R., and Wilcke, R. A.: VALUE: A framework to validate downscaling approaches for climate change studies, Earth's Future, 3, 1–14, 2015.

Meredith, E. P., Rust, H. W., and Ulbrich, U.: A classification algorithm for selective dynamical downscaling of precipitation extremes, Hydrology and Earth System Sciences, 22, 4183–4200, 2018.

Mitchell, T. D. and Hulme, M.: Predicting regional climate change: living with uncertainty, Progress in Physical Geography, 23, 57–78, 1999.

Muttaqien, F. H., Rahadianti, L., and Latifah, A. L.: Downscaling for Climate Data in Indonesia Using Image-to-Image Translation Approach, in: 2021 International Conference on Advanced Computer Science and Information Systems (ICACSIS), pp. 1–8, IEEE, 2021.

Naddaf, M.: Climate change is costing trillions-and low-income countries are paying the price., Nature, 2022.

Panitz, H.-J., Dosio, A., Büchner, M., Lüthi, D., and Keuler, K.: COSMO-CLM (CCLM) climate simulations over CORDEX-Africa domain: analysis of the ERA-Interim driven simulations at 0.44 and 0.22 resolution, Climate dynamics, 42, 3015–3038, 2014.

Qiu, Y., Feng, J., Yan, Z., and Wang, J.: HCPD-CA: high-resolution climate projection dataset in central Asia, Earth System Science Data, 14, 2195–2208, 2022.

Racah, E., Beckham, C., Maharaj, T., Ebrahimi Kahou, S., Prabhat, M., and Pal, C.: Extremeweather: A large-scale climate dataset for semi-supervised detection, localization, and understanding of extreme weather events, Advances in neural information processing systems, 30, 2017.

Rampal, N., Hobeichi, S., Gibson, P. B., Baño-Medina, J., Abramowitz, G., Beucler, T., González-Abad, J., Chapman, W., Harder, P., and Gutiérrez, J. M.: Enhancing Regional Climate Downscaling through Advances in Machine Learning, Artificial Intelligence for the Earth Systems, 3, 230 066, 2024.

This page contains no comments

Randall, D. A., Wood, R. A., Bony, S., Colman, R., Fichefet, T., Fyfe, J., Kattsov, V., Pitman, A., Shukla, J., Srinivasan, J., et al.: Climate models and their evaluation, in: Climate change 2007: The physical science basis. Contribution of Working Group I to the Fourth Assessment Report of the IPCC (FAR), pp. 589–662, Cambridge University Press, 2007.

585 Reichstein, M., Camps-Valls, G., Stevens, B., Jung, M., Denzler, J., Carvalhais, N., and Prabhat, f.: Deep learning and process understanding for data-driven Earth system science, Nature, 566, 195–204, 2019.

Reyer, C. P., Otto, I. M., Adams, S., Albrecht, T., Baarsch, F., Cartsburg, M., Coumou, D., Eden, A., Ludi, E., Marcus, R., et al.: Climate change impacts in Central Asia and their implications for development, Regional Environmental Change, 17, 1639–1650, 2017.

Riahi, K., Van Vuuren, D. P., Kriegler, E., Edmonds, J., O'neill, B. C., Fujimori, S., Bauer, N., Calvin, K., Dellink, R., Fricko, O., et al.: The
590 shared socioeconomic pathways and their energy, land use, and greenhouse gas emissions implications: an overview, Global environmental change, 42, 153–168, 2017.

Rockel, B. and Geyer, B.: The performance of the regional climate model CLM in different climate regions, as simulated in a transient climate change experiment, Climate Dynamics, 31, 713–728, 2008.

Rummukainen, M.: State-of-the-art with regional climate models, Wiley Interdisciplinary Reviews: Climate Change, 1, 82–96, 2010.

595 Russo, E., Kirchner, I., Pfahl, S., Schaap, M., and Cubasch, U.: Sensitivity studies with the regional climate model COSMO-CLM 5.0 over the CORDEX Central Asia Domain, Geoscientific Model Development, 12, 5229–5249, 2019.

Russo, E., Sørland, S. L., Kirchner, I., Schaap, M., Raible, C. C., and Cubasch, U.: Exploring the parameter space of the COSMO-CLM v5. 0 regional climate model for the Central Asia CORDEX domain, Geoscientific Model Development, 13, 5779–5797, 2020.

Russo, E., Fallah, B., Ludwig, P., Karremann, M., and Raible, C. C.: The long-standing dilemma of European summer temperatures at
600 the mid-Holocene and other considerations on learning from the past for the future using a regional climate model, Climate of the Past Discussions, 2021, 1–27, 2021.

Sørland, S. L., Schär, C., Lüthi, D., and Kjellström, E.: Bias patterns and climate change signals in GCM-RCM model chains, Environmental Research Letters, 13, 074 017, 2018.

Sørland, S. L., Brogli, R., Pothapakula, P. K., Russo, E., Van de Walle, J., Ahrens, B., Anders, I., Bucchignani, E., Davin, E. L., Demory,
605 M.-E., et al.: COSMO-CLM regional climate simulations in the Coordinated Regional Climate Downscaling Experiment (CORDEX) framework: a review, Geoscientific Model Development, 14, 5125–5154, 2021.

Taylor, K. E., Stouffer, R. J., and Meehl, G. A.: An overview of CMIP5 and the experiment design, Bulletin of the American meteorological Society, 93, 485–498, 2012.

Volosciuk, C., Maraun, D., Vrac, M., and Widmann, M.: A combined statistical bias correction and stochastic downscaling method for
610 precipitation, Hydrology and Earth System Sciences, 21, 1693–1719, 2017.

Wang, D., Menz, C., Simon, T., Simmer, C., and Ohlwein, C.: Regional dynamical downscaling with CCLM over East Asia, Meteorology and Atmospheric Physics, 121, 39–53, 2013.

Wang, X., Otto, M., and Scherer, D.: Atmospheric triggering conditions and climatic disposition of landslides in Kyrgyzstan and Tajikistan at the beginning of the 21st century, Natural Hazards and Earth System Sciences, 21, 2125–2144, 2021.

615 Watson-Parris, D., Rao, Y., Olivié, D., Seland, Ø., Nowack, P., Camps-Valls, G., Stier, P., Bouabid, S., Dewey, M., Fons, E., et al.: ClimateBench v1. 0: A benchmark for data-driven climate projections, Journal of Advances in Modeling Earth Systems, 14, e2021MS002 954, 2022.

Xu, P., Wang, L., and Ming, J.: Central Asian precipitation extremes affected by an intraseasonal planetary wave pattern, Journal of Climate, 35, 2603–2616, 2022.

This page contains no comments

620 Xu, Z., Han, Y., Tam, C.-Y., Yang, Z.-L., and Fu, C.: Bias-corrected CMIP6 global dataset for dynamical downscaling of the historical and
       future climate (1979–2100), Scientific Data, 8, 293, 2021.

Yan, Y., You, Q., Wu, F., Pepin, N., and Kang, S.: Surface mean temperature from the observational stations and multiple reanalyses over the
       Tibetan Plateau, Climate Dynamics, 55, 2405–2419, 2020.

Zhu, X. X., Tuia, D., Mou, L., Xia, G.-S., Zhang, L., Xu, F., and Fraundorfer, F.: Deep learning in remote sensing: A comprehensive review
625   and list of resources, IEEE geoscience and remote sensing magazine, 5, 8–36, 2017.

This page contains no comments